Applied Energy 377 (2025) 124659

Contents lists available at ScienceDirect

Applied Energy

journal homepage: www.elsevier.com/locate/apenergy

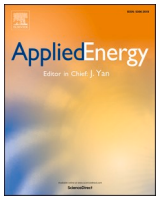

A two-layer strategy for sustainable energy management of microgrid clusters with embedded energy storage system and demand-side flexibility provision

Farid Moazzen [a], M.J. Hossain [a,*]

[a] School of Electrical and Data Engineering, University of Technology Sydney, NSW, Australia

HIGHLIGHTS

- Two-layer energy management strategy optimizes clustered microgrids' operations.
- Demand-side flexibility and shared battery storage cut costs and reduce emissions.
- Mixed-integer quadratic programming (MIQP) ensures optimal scheduling accuracy.
- Case studies show 6.9 % cost savings using real data from Australian microgrids.
- The model supports net-zero energy decisions and sustainable grid management.

ARTICLE INFO

Keywords:
Energy management
Optimization
Storage system
MIQP
Microgrid cluster

ABSTRACT

The intermittent nature of renewable energy generation and the fluctuating demands pose persistent challenges in microgrid operations. In response, stakeholders and operators have turned to clustering the geographically adjacent microgrids as a solution. In this context, this paper introduces a novel two-layer energy management strategy for microgrid clusters, utilizing demand-side flexibility and the capabilities of shared battery energy storage (SBES) to minimize operational costs and emissions, while ensuring a spinning reserve within individual microgrids to prevent load-shedding. In the lower layer, the proposed approach devises optimal day-ahead operation policies, while the upper layer employs a cooperative strategy to further optimize the operational efficiency across the entire cluster. The energy management problem is accurately formulated as a mixed integer quadratic programming (MIQP) optimization, which incorporates linear terms in the problem's constraints. The formulation accounts for operational costs associated with SBES including expenses of charging/discharging and changes in operating states (CiOS). Real-world case studies with a cluster of three microgrids in Australia validate the effectiveness of this approach. Results show a reduction in operational costs for the base case scenario by 6.96 % compared to conventional microgrid management strategies. Sensitivity analyses further demonstrate the economic benefits of varying SBES capacity and flexibility pricing, with savings ranging from 6.5 % to 8.1 %. The proposed strategy also reduces CO2 emissions by up to 11.6 %, while improving system reliability. This strategy holds promise for integration into distributed energy systems with high renewable penetration and clustered local grids, offering significant advantages for utility operators and end-users through improved energy efficiency and reduced emissions.

1. Introduction

The microgrid concept, emerging as a focal point of innovation, has recently evolved to encompass multi-microgrid systems that offer superior reliability by leveraging mutual support during periods of generation shortfalls or heightened demand, stemming from the intermittent nature of renewable energy sources. Interconnecting microgrids as clusters not only bolsters reliability but also opens up diverse avenues for enhanced economic viability. By harnessing synergies among clustered microgrids, operators can optimize resource distribution and trading prospects, thereby maximizing economic benefits. Moreover,

* Corresponding author.
E-mail address: jahangir.hossain@uts.edu.au (M.J. Hossain).

https://doi.org/10.1016/j.apenergy.2024.124659
Received 26 May 2024; Received in revised form 10 September 2024; Accepted 5 October 2024
Available online 17 October 2024

Nomenclature

h	Time index (hour of the day)
i	The index of ith CGUs
j	The index of jth BES
k	The index of kth PV
m	The index of microgrid
$\lambda^{imp}_{m,h}$, $\lambda^{exp}_{m,h}$	The binary indicators of energy import and export of mth microgrid at hour h
$E^{imp}_{m,h}$, $E^{exp}_{m,h}$	The imported and exported energy by mth microgrid at hour h
$\varphi^{imp}_{m,h}$, $\varphi^{exp}_{m,h}$	The unit prices of buying and selling electricity by mth microgrid from/to an adjacent microgrid at hour h
$P^{imp}_{m,min}$, $P^{imp}_{m,max}$	The import and export power limits for mth microgrid
λ^{buy}_{h}, λ^{sell}_{h}	The binary indicators of buying and selling from/to the grid at hour h
E^{buy}_{h}, E^{sell}_{h}	The electricity bought and sold from/to the main grid at hour h
P^{buy}_{max}, P^{sell}_{max}	The maximum power import and export from the grid
φ^{buy}_{h}, φ^{sell}_{h}	The electricity unit price for buying/selling from the main grid at hour h
$E^{CGU}_{i,h}$	The output energy(kWh) of ith CGU at hour h
$P^{CGU}_{i,min}$, $P^{CGU}_{i,max}$	The minimum and capacity/maximum power output rate of the ith CGU
a^{CGU}_{i}, b^{CGU}_{i}, c^{CGU}_{i}	The coefficients of ith CGU cost model
R^{CGU}_{i}	The generation ramp rate of CGUs
$E^{BES}_{j,h}$	The output energy(kWh) of jth BES at hour h
Cap^{BES}_{j}/ Cap^{SBES}_{max}	The maximum energy capacity of jth battery/SBES
α^{BES}_{j}, β^{BES}_{j}	The coefficients of jth BES cost model
γ^{ch}_{h}, γ^{dch}_{h}	The binary indicator of charging/discharging the battery at hour h
$SoC_{j,h}$	The remaining charge (state of charge) of jth BES at hour h
$\alpha^{BES}_{j,min}$, $\beta^{BES}_{j,max}$	The coefficient to limit the jth BES minimum/maximum SoC
$\eta^{BES}_{j,ch}$, $\eta^{BES}_{j,dch}$	The charging/discharging efficiency of ith BES
$NCiOS^{BES}_{j}$	The number of changes in operating state of Jth BES
$NCiOS^{BES}_{j,max}$	The maximum number of changes in operating state of Jth BES
$CiOS^{BES}_{j,h}$	Indicator of the operating state changing at hour h of Jth BES
ξ	An auxiliary parameter in the set of real numbers
ρ_{j}	Cost of each alteration in the operating state of Jth BES
$E^{PV}_{k,h}$	The output energy (kWh)/power(kW) at hour h
$P^{PV}_{k,max}$	The capacity/maximum power output rate of the kth PV
$I^{PV}_{k,crt}$	The certain radiation (kW/m^2) of the kth PV
$I^{PV}_{k,std}$	The standard solar radiation (kW/m^2) of the kth PV
$I^{PV}_{k,h}$	The solar radiation intensity (kW/m^2) of the kth PV at hour h
σ_{k}	The coefficient of kth PV (RESs) cost model
L^{C-EMS}_{h}, G^{C-EMS}_{h}	Net MC load and generation observed by C-EMS
E^{flex}_{h}, E^{inflex}_{h}	The flexible and inflexible load for individual microgrids
L^{flex}_{h}	The total flexibility provision for C-EMS
$L^{flex}_{h,app}$, $L^{flex}_{h,unapp}$	The applied and unapplied portions of the flexibility provision
(I-/C-) EMS	(Individual microgrid's/ The Cluster's) Energy Management System
MG	Microgrid
MC	Microgrid Cluster
PCC	Point of Common Coupling
MPSC	Mixed Parallel-Series Connection
MIQP	Mixed-integer Quadratic Programming
(S) BES	(Shared) Battery Energy Storage
DSO	Distribution System Operator
SoC	State of Charge,
CGU	Conventional Generation Unit
PV	Photovoltaic generation unit
(N)CiOS	(The number of) Changes in Operating State
CO2e	CO2 equivalent

microgrid clusters offer several technical advantages, including resource and energy exchange among constituent microgrids to ensure stable operation through self-healing capabilities, diminish dependence on local generation, mitigate load curtailment, enhance the utilization of renewable energy, and augment grid reliability [1–4]. These technical merits have spurred practical deployments of such systems. To provide an example, the Illinois Institute of Technology has deployed a DC multi-microgrid for analyzing economic dispatching. Furthermore, the U.S. Department of Energy is developing a central controller to integrate the Bronzeville community microgrid with the Illinois Institute of Technology campus microgrid [5].

In numerous instances, existing distribution networks primarily rely on fossil fuels; however, with the imposition of penalties for CO2 emissions, there is now a concerted push towards renewable generation.

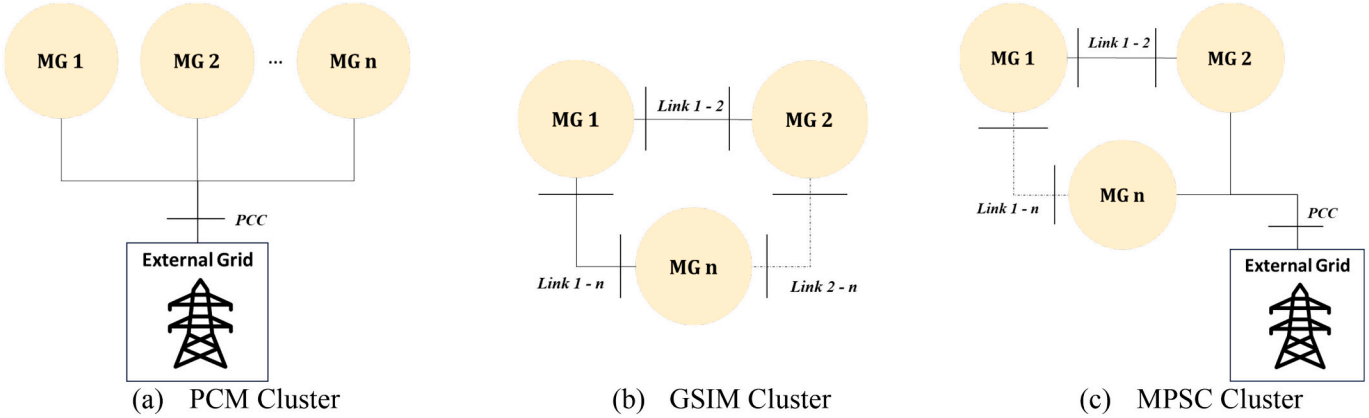

Fig. 1. Illustrative diagram of the common architectures for microgrid clusters.

This shift is anticipated to result in a notable rise in distributed generation installations. Nonetheless, integrating these new units presents challenges such as their intermittent behaviour for system operation, particularly given that the distributed system operator may not possess adequate capabilities to manage them all effectively. To address similar challenges in a cost-efficient manner, clustering microgrids is expected as a viable solution [6]. The technology of microgrid clusters (MCs) is advancing through the interconnection of multiple geographically adjacent microgrids, with the overarching objective of enhancing overall system reliability and energy utilization efficiency. Microgrid clusters confer economic advantages by lowering costs for end-users, mitigating active losses, and reducing emissions [7]. In scenarios characterized by microgrids possessing surplus energy, the concept of clustering proves advantageous as they can collaborate with microgrids facing energy deficits by efficiently exchanging excess energy. Various architectural configurations for microgrid clusters are discussed in [6,8]. The most common configurations include Parallel Connected Microgrids (PCM), where all microgrids are linked to an external grid, and any power exchange between microgrids must pass through the external grid to enable power flow and ancillary services. Another configuration is Grid Series Interconnected Microgrids (GSIM), where microgrids are directly connected, forming a cluster that enhances system resilience, though it requires careful coordination to maintain voltage and frequency stability in islanded mode. A hybrid approach, the Mixed Parallel-Series Connection (MPSC), combines aspects of both PCM and GSIM, with some microgrids connected to the external grid and others linked via point-to-point connections. This arrangement increases flexibility and allows microgrids to support each other during isolated operations, making it a particularly promising option [8]. Fig. 1 presents diagrammatic representations of these common microgrid cluster architectures.

Amidst the dynamic landscape of microgrid clusters, the indispensable role of energy management systems remains paramount. These systems act as pivotal components, orchestrating the intricate interplay between economic and technical factors that govern microgrid operations. Energy management encompasses the strategic layer of microgrid control, while power management and local controls function at the tactical level. Thus, the choice of a proficient energy management strategy emerges as a crucial determinant, directly influencing the profitability of stakeholders and the contentment of demand-side entities.

Examining the concept of energy management in microgrid clusters, a robust energy management strategy for interconnected microgrids is proposed in [9], leveraging distributed optimization techniques. However, this approach overlooks the operating costs associated with energy storage, including degradation. In [10] the authors introduce a decomposed optimization formulation to tackle energy sharing and payment bargaining allocation within grid-connected microgrids. Despite incorporating Generalized Nash Bargaining and peer-to-peer communication for privacy, the model lacks a complete representation of storage systems, potentially resulting in unforeseen expenses. A fully decentralized energy management approach based on a transactive energy framework is proposed in [11]. Although this method optimizes operational costs and market clearing prices using distributionally robust optimization, its practical implementation may face challenges due to the requirement for extensive equipment installation. In [12], an Energy Management System (EMS) framework for multi-microgrids is presented, considering uncertainties through affine forms and noise symbols. However, the degradation cost of batteries is not considered. Addressing the optimization of pricing policies to synchronize multiple microgrids within distribution networks, authors in [13] convert the bi-level system into a Markov Decision Process and refine the pricing strategy. Nonetheless, there remains scope for presenting a more precise model, as the authors employ a model-free approach.

An integrated model of microgrid energy management and demand response initiatives considering storage systems are presented by the author in [14] for a single microgrid operation neglecting the capability of clustering microgrids. The energy management framework proposed in [15] for off-grid microgrid clusters, utilizes tube model predictive control to optimize energy scheduling while minimizing economic trade-offs; however, it does not account for transactions with the main grid or incorporate considerations of load demand flexibility. Researchers in [16], employ a multi-level optimization model to facilitate coordinated energy management across microgrids and clustered microgrids at the lower level, and between clusters and distribution systems, as well as upstream networks at the upper level. Nonetheless, the study overlooks the potential of embedded energy storage systems shared between clusters. The research in [17] devises an EMS using a multi-step hierarchical decentralized strategy for a cluster of interconnected isolated microgrids, albeit neglecting embedded energy storage systems. Additionally, authors in [18] utilize a battery storage logistic model to introduce an EMS model for microgrid clusters. Notably, both studies focused on microgrid clusters operating independently, overlooking grid exchange capability.

After reviewing the existing literature, it becomes evident that embedded storage systems, especially within microgrid clusters, have been largely overlooked. Furthermore, there is a gap in the exploration of computationally efficient methods that encompass the complete model of energy storage systems while employing precise mathematical formulations. Additionally, the importance of limiting data transmission for crafting effective energy management strategies is sometimes disregarded. Moreover, there exists limited discourse on sustainable solutions that aim to minimize load shedding while prioritizing low carbon emissions. In light of these observations, this study proposes a novel approach where a cluster of microgrids invests in a shared storage system to minimize operational costs. This approach involves treating renewable power generation as non-schedulable and integrating it into the system, with each microgrid paying a regulator-set tariff separate from the market clearing price. The primary contributions of this paper can be summarized as follows:

- Proposing a two-layer energy management strategy for geographically adjacent microgrids entails the development of accurate mathematical formulations for energy storage systems utilizing the Mixed-Integer Quadratic Programming (MIQP) approach. This approach incorporates linear constraints to facilitate the identification of the exact optimal solution.
- Incorporating demand-side flexibility into the cluster's energy management system (C-EMS) to enable cooperation between microgrids and reduce operational costs. It also helps minimize carbon emissions from fossil-based generation, whether local or grid-side, aligning with sustainability objectives while enhancing overall reliability.
- Embedding a shared Battery Energy Storage (BES) system serves to mitigate the intermittency of renewable power generation and address supply deficiencies. This shared BES enables clustered microgrids to collaborate in meeting neighbouring microgrids' demands across different time intervals.
- Formulating the cost associated with battery operation mode alteration within the microgrid's EMS in addition to considering battery degradation costs attributed to charging or discharging, as well as the investment cost related to battery lifespan. This consideration is crucial to preempt unexpected expenses, particularly stemming from changes in the current direction of batteries.

The following sections of this paper are organized as follows: Section 2 introduces the methodology framework and system architecture. In Section 3, an in-depth exploration of the proposed energy management strategy is provided, which encompasses the formulation of optimization problems and a sustainable decision-making process designed to attain the global optimal solution. Section 4 focuses on the methodology used for solving these problems, while Section 5 presents the numerical

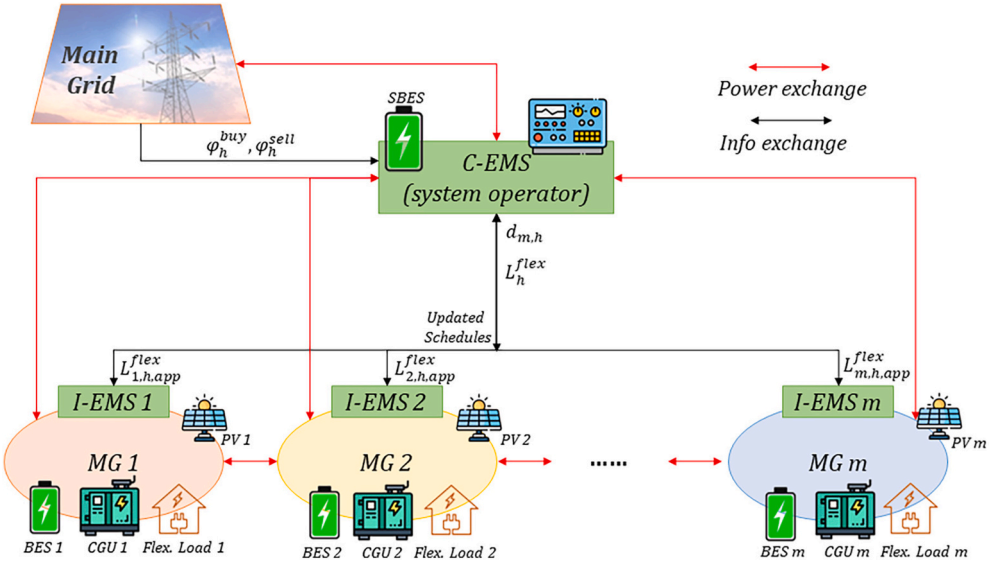

Fig. 2. Illustrative diagram of the microgrid cluster

findings and ensuing discussions. Lastly, Section 6 encapsulates the paper with concluding remarks.

2. The system architecture and modeling

This section introduces the methodology framework of the study, providing an overview of the system components and the mathematical formulation governing the EMS. The study focuses on a cluster of interconnected microgrids, each equipped with its own EMS designed to optimize the operation schedules of energy generation and consumption based on day-ahead forecasted data. These microgrids are connected to C-EMS, which supervises energy storage using a shared battery energy storage (SBES) system, enhancing the reliability and flexibility of individual microgrids. Each microgrid consists of its battery energy storage (BES), renewable energy generation (such as photovoltaic systems), and conventional fossil fuel-based generation units. The system can operate in either grid-connected or isolated modes, with C-EMS coordinating power exchanges with the grid to minimize costs and optimize efficiency. Fig. 2 illustrates the system with MPSC architecture, depicting power flows within and between microgrids and C-EMS. Microgrid load flexibility is collectively managed in a cooperative manner, with considerations given to the minimum state of charge of BESs to prevent complete depletion for the sake of maintaining battery performance as well as to provide a spinning reserve for supporting reliability. Energy transactions occur between neighbouring microgrids and between the C-EMS and the main grid, aiming to minimize overall operational costs while considering load flexibility and energy storage capabilities for future intervals. Notably, the transmission of data to the system operator (C-EMS) is limited, ensuring the confidentiality of microgrid information and enhancing security measures. The subsequent section outlines the mathematical formulation governing the system's operation.

3. Proposed two-layer energy management strategy

The two-layer energy management strategy is designed to leverage microgrid synergies to enhance overall system efficiency. A centralized EMS possesses the capability to integrate diverse storage systems, encompassing battery storage, hydrogen storage, and electric vehicle

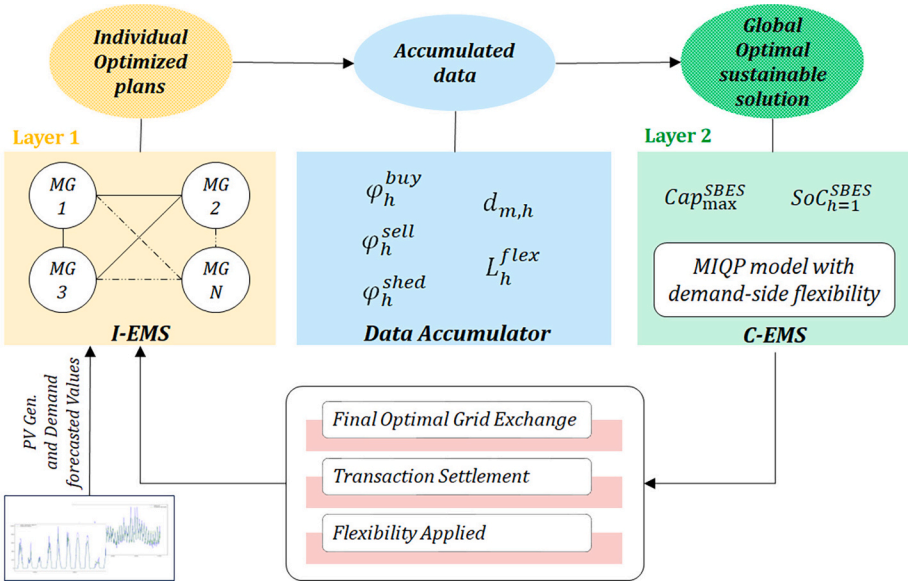

Fig. 3. The procedure of the two-layer energy management strategy.

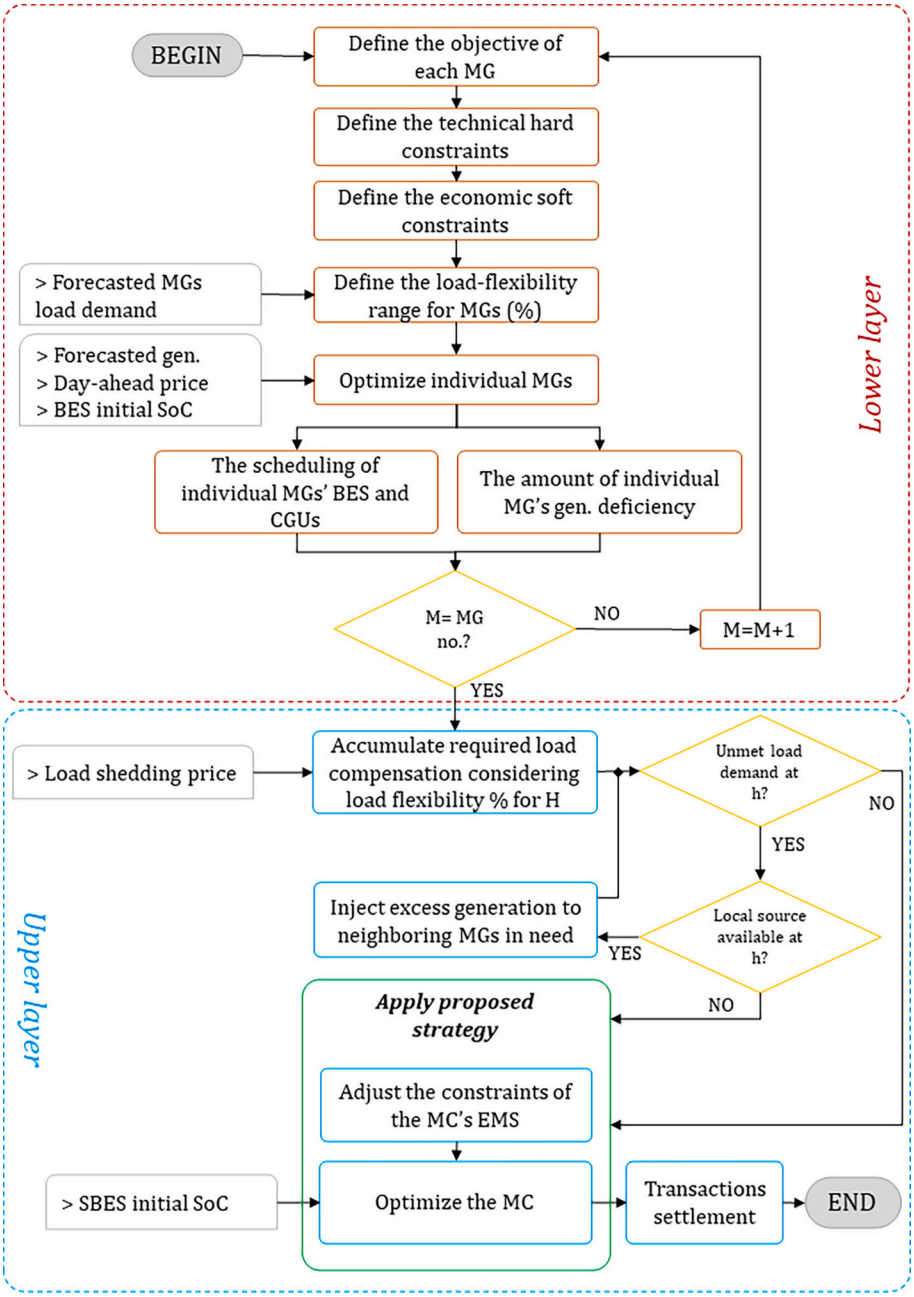

Fig. 4. The flowchart of the two-layer energy management strategy for the MC.

aggregators. This paper specifically focuses on the modeling aspect of BESs. Each individual microgrid's EMS (I-EMS) optimizes the schedule of its associated microgrid, which is then coordinated by C-EMS. The C-EMS optimizes the entire system, considering factors such as generation deficiencies, load flexibility, excess generation available for export, and storage system capabilities across different time intervals. After optimizing the system, the C-EMS facilitates transaction settlements to ensure the optimal operation of individual microgrids. From the Distribution System Operator's (DSO) viewpoint, C-EMS operates as a price-taker. This means that the electricity price between the C-EMS and the DSO remains unchanged by the scheduling strategy and is merely determined by the electricity market. Fig. 3 visually represents the proposed two-layer strategy, whereas Fig. 4 presents a flowchart detailing the proposed strategy. The following subsections delineate both the lower layer and upper layer of the procedure.

3.1. The lower layer: Optimization problem formulation for microgrids

Layer 1 of the proposed strategy focuses on optimizing individual microgrids, with each microgrid targeting a specific goal for its exchange schedule. In this study, the primary objective is to minimize operational costs. Once each microgrid has optimized its schedule to achieve this goal, it submits the optimized schedule to the upper layer. Each microgrid comprises a conventional generation unit (CGU), battery storage system (BES), and photovoltaic generation unit (PV) to meet specific load demands. To execute this layer, the mathematical formulations are presented below. The inputs for this layer include the generation capacity and specifications of the CGU, PV, and BES, along with the initial state of charge (SoC) of the BES. Furthermore, the individual EMSs must be provided with forecasted market prices for electricity, irradiance, and load demand. The optimization process of layer 1 produces outputs consisting of the day-ahead hourly generation schedule

and the SoC of BESs. According to [19–22] the mathematical cost model can be developed as follows.

- The Model for Conventional Generation Units:

According to the literature, the model for natural gas generators, referred to here as CGUs, can be calculated as follows:

$$Cost^{CGU} = \sum_{i=1}^{CGU}\sum_{h=1}^{H} a_i^{CGU}\left(\mathrm{E}_{i,h}^{CGU}\right)^2 + b_i^{CGU}\left(\mathrm{E}_{i,h}^{CGU}\right) + c_i^{CGU} \quad (1)$$

Where a_i^{CGU}, b_i^{CGU}, and c_i^{CGU} are the i^{th} CGU coefficients and $E_{i,h}^{CGU}$ denotes its output energy at hour h. The operation of CGUs in the optimization model should satisfy the following constraints which relate to minimum and maximum generation capacity, and ramp rate limits, respectively. It is worth mentioning that when the CGU operates continuously at least at the minimum generation level of $P_{i,min}^{CGU}$, the need to consider shutdown or startup costs is eliminated:

$$P_{i,min}^{CGU} \le E_{i,h}^{CGU} \le P_{i,max}^{CGU} \quad (2)$$

$$E_{i,h-1}^{CGU} - R_i^{CGU} \le E_{i,h}^{CGU} \le E_{i,h-1}^{CGU} + R_i^{CGU} \quad (3)$$

Where $P_{i,min}^{CGU}$ and $P_{i,max}^{CGU}$ represent the minimum and maximum power output rate of i^{th} CGU, respectively.

- The RES (PV) Model:

The operational expenses of photovoltaic (PV) systems primarily comprise maintenance costs, which are generally unrelated to the generated power quantity. However, in assessing the operational cost of renewable energy sources (RES) such as PV, a nominal constant coefficient is typically applied to the power output during operational intervals.

$$Cost^{PV} = \sum_{k=1}^{K}\sum_{h=1}^{H} \sigma_k . E_{k,h}^{PV} \quad (4)$$

$$\begin{cases} \dfrac{\left(I_{k,h}^{PV}\right)^2}{I_{k,std}^{PV}.I_{k,crt}^{PV}} & if \quad 0 \le I_{k,h}^{PV} < I_{k,crt}^{PV} \\ \dfrac{I_{k,h}^{PV}}{I_{k,std}^{PV}} & if \quad I_{k,crt}^{PV} \le I_{k,h}^{PV} < I_{k,std}^{PV} \\ 1 & if \quad I_{k,std}^{PV} \le I_{k,h}^{PV} \end{cases} \quad (5)$$

$$P_{total,min}^{PV} \le \sum_{k=1}^{PV}\sum_{h=1}^{H} E_{k,h}^{PV} \quad (6)$$

Where $E_{k,h}^{PV}$ is the output power at hour h and σ_k is the coefficient of k^{th} *PV unit.* $I_{k,h}^{PV}$, $I_{k,crt}^{PV}$, $I_{k,std}^{PV}$ represent the solar radiation intensity, the certain radiation, and the standard solar radiation, respectively.

- The energy exchange within the system

The mathematical cost model governing energy exchange within an interconnected system of microgrids encompasses the formulation aimed at precisely quantifying the economic ramifications associated with energy transactions between these microgrids. As elucidated by **Eq. (7)**, the cost of energy exchange for Microgrid m can be computed as the disparity between the energy imported by the EMS and the energy exported either from/to neighbouring microgrids or from/to the main grid. It is imperative to underscore that at this phase of the energy management strategy, the optimal operation of the microgrid is determined by considering the total exchanges, with the subsequent phase accounting for the eventual optimal energy exchange with the main grid.

$$Cost_m^{exchange} = \sum_{h=1}^{H}\left(\lambda_{m,h}^{imp}E_{m,h}^{imp}\varphi_{m,h}^{imp} - \lambda_{m,h}^{exp}E_{m,h}^{exp}\varphi_{m,h}^{exp}\right) \quad (7)$$

In this equation, $E_{m,h}^{imp}$, $E_{m,h}^{exp}$ denote the imported and exported energy, respectively, while $\varphi_{m,h}^{imp}$, $\varphi_{m,h}^{exp}$ represent unit prices of buying and selling electricity of the m^{th} microgrid at hour h, respectively. The binary variables (λ) help the optimization process enable or disable the microgrid external transactions. As indicated in (8) and (9), the maximum practical power limits ($P_{m,max}^{imp}$, $P_{m,max}^{exp}$) restrict the amount of imported or exported electricity of the m^{th} microgrid.

$$\lambda_{m,h}^{imp}.E_{m,h}^{imp} \le P_{\mathrm{m},max}^{imp} \quad (8)$$

$$\lambda_{m,h}^{exp}.E_{m,h}^{exp} \le P_{\mathrm{m},max}^{exp} \quad (9)$$

- Battery Energy Storage (BES) System Model:

The mathematical representation of a BES within a microgrid EMS entails the consideration of various factors crucial for comprehensively capturing its behaviour and influence on energy optimization. Typically, this modeling approach, shown in Eq. (10) incorporates key parameters such as the battery's SoC, charging and discharging rates, efficiency, and capacity constraints. These factors are often expressed through mathematical formulations derived from fundamental principles and empirical observations. Furthermore, the operational behaviour of the battery within the microgrid EMS is governed by constraints related to its capacity, charge/discharge rates, and maximum/minimum state of charge. Additionally, the model may account for aging effects resulting from continuous changes in operational conditions, which contribute to the degradation of the BES over time, thereby enhancing the model's accuracy and reliability. **Eq. (10)** represents the cost model of BESs.

$$Cost^{BES} = Cost_j^{BES,ch/dch} + Cost_j^{BES,\mathrm{OS}} \quad (10)$$

In **Eq. (10)**, the BES operation costs include the battery degradation cost due to charging and discharging, as well as the costs associated with changes in the operating state or current direction. **Eq. (11)** calculates the cost of charging/discharging of j^{th} BES which refers to the battery degradation stemming from charging or discharging:

$$Cost_j^{BES,ch/dch} = \sum_{h=1}^{H}\left(\alpha_j^{BES}\left(\mathrm{E}_{j,h}^{BES}\right)^2 + \beta_j^{BES}\right) \quad (11)$$

Where α_j^{BES} *and* β_j^{BES} are the j^{th} BES's coefficients and $E_{j,h}^{BES}$ denotes the output energy at hour h. Battery degradation is the gradual reduction in a battery's ability to store and release energy over time. This process inevitably leads to decreased energy capacity, range, power output, and overall efficiency of the device it powers. Therefore, the constant coefficients are set in a way that considers the cost of capacity fading and the present value of battery replacement cost. The cost associated with not utilizing the battery system during periods of zero charging or discharging, when the charging rate is also zero, is computed by the intercept of β_j^{BES}. Moreover, the second term in Eq. (10), which accounts for changes in the operating state (CiOS), incurs an associated cost that is calculated as follows:

$$CiOS_{j,h}^{BES} = sign\left[sign\left(E_{j,h}^{BES}\right) - sign\left(E_{j,h-1}^{BES}\right)\right] \quad (12)$$

$$\begin{cases} \lim\limits_{x\to 0^-} sign(x) = -1 \\ \lim\limits_{x\to 0^+} sign(x) = 1 \end{cases} \quad (13)$$

$$sign(x) \approx tanh(\xi.x), \xi \in \mathbb{R}$$

$$CiOS_{j,h}^{BES} = tanh\left(\xi\left[tanh\left(\xi E_{j,h}^{BES}\right) - tanh\left(\xi E_{j,h-1}^{BES}\right)\right]\right) \quad (14)$$

$$Cost_j^{BES,OS} = \rho_j.\left(\sum_{h=1}^{H-1}\left|CiOS_{j,h}^{BES}\right|\right) = \rho_j.\left(\sum_{h=1}^{H-1}\left(tanh\left(\xi\left[tanh\left(\xi E_{j,h}^{BES}\right) - tanh\left(\xi E_{j,h-1}^{BES}\right)\right]\right)\right)\right) \quad (15)$$

It should be noted that the *sign(.)* function yields different values for negative zero and positive zero (0^-,0^+). To address this issue when dealing with *sign(0)*, the tanh*(.)* function is employed with a large real coefficient as an auxiliary parameter (ξ). Each BES's operation is subject to the constraints **(16)** to **(18)**, showing the output rate limits ($P_{j,max}^{BES,ch}$, $P_{j,max}^{BES,dch}$), avoiding charging/discharging at the same time by utilizing the binary variables γ_h^{ch} and γ_h^{dch}, and the boundaries of batteries' SoC ($SoC_{j,min}$, $SoC_{j,max}$), which are to increase the lifetime and decrease aging. It is important to highlight that positive values denote discharging, while negative values denote charging, as the BES is regarded as an energy source rather than a demand.

$$P_{j,max}^{BES,ch} \le E_{j,h}^{BES} \le P_{j,max}^{BES,dch} \quad (16)$$

$$\gamma_h^{ch} + \gamma_h^{dch} = 1 \quad (17)$$

$$SoC_{j,min} \le SoC_{j,h} \le SoC_{j,max} \quad (18)$$

In addition, the remaining charge of BES or the SoC for the next hour can be calculated by **(19)**. In this equation, $\eta_{j,ch}^{BES}$ and $\eta_{j,dch}^{BES}$ indicate the charging and discharging efficiency of j^{th} BES, respectively, while Cap_j^{BES} refers to its maximum energy capacity.

$$SoC_h = SoC_{h-1} + \eta_{j,ch}^{BES}\left(\gamma_h^{ch}\frac{E_{j,h}^{BES}}{Cap_j^{BES}}\right) - \frac{1}{\eta_{j,dch}^{BES}}\left(\gamma_h^{dch}\frac{E_{j,h}^{BES}}{Cap_j^{BES}}\right) \quad (19)$$

To limit the number of CiOS (NCiOS) of BESs another constraint can be applied:

$$\frac{1}{H}NCiOS_j^{BES} = \frac{1}{H}\sum_{h=1}^{H-1}\left|CiOS_{j,h}^{BES}\right| \le \frac{1}{H}NCiOS_{j,max}^{BES}, \forall BESs \quad (20)$$

- Objective Function(s)

The objective function governing the optimization of operational strategies to minimize costs while ensuring a reliable power supply is formulated by **Eq. (21)**. It encompasses considerations such as exchange-related expenses, generation costs, and BES operational costs to attain optimal economic performance.

$$OF-I: min \times \sum_{h=1}^{H}\left\{\left(Cost^{exchange} + \sum_{i=1}^{CGU}Cost_i^{CGU} + \sum_{j=1}^{BES}Cost_j^{BES,ch/dch} + \sum_{k=1}^{PV}Cost_k^{PV}\right)\right. \quad (21)$$

$$\text{OF}-\text{I}: \left(\lambda_{m,h}^{imp}.E_{m,h}^{imp}.\varphi_{m,h}^{imp} - \lambda_{m,h}^{exp}.E_{m,h}^{exp}.\varphi_{m,h}^{exp}\right) + \sum_{i=1}^{CGU}\left(a_i^{CGU}\left(E_{i,h}^{CGU}\right)^2 + b_i^{CGU}\left(E_{i,h}^{CGU}\right) + c_i^{CGU}\right) + \sum_{j=1}^{BES}\left(\alpha_j^{BES}\left(E_{j,h}^{BES}\right)^2 + \beta_j^{BES}\right) + \sum_{k=1}^{PV}\sigma_k.E_{k,h}^{PV} \quad (22)$$

while $\lambda_{m,h}^{imp}$, $E_{m,h}^{imp}$, $\lambda_{m,h}^{exp}$, $E_{m,h}^{exp}$, $E_{i,h}^{CGU}$, $E_{j,h}^{BES}$, $\gamma_{j,h}^{ch}$, $\gamma_{j,h}^{dch}$, $E_{k,h}^{PV}$ are the decision variables.

- Problem Constraints

The objective function described above dynamically adjusts to varying energy demands, renewable energy availability, and market prices, facilitating efficient resource utilization while adhering to operational constraints. Among these constraints, the most crucial, referred to as a hard constraint, is maintaining the power balance between generation and consumption across the entire network shown by **Eq. (23)**, accounting for energy exchanges with the grid. In this context, the load demand is deemed partially flexible, comprising both flexible and inflexible or critical components as depicted by **Eq. (24)**. The flexible portion can be adjusted or curtailed if necessary, while the inflexible or critical segment must be supplied without interruption.

$$E_h^{Load} + \gamma_h^{ch}\sum_{j=1}^{BES}E_{j,h}^{BES,ch} + \lambda_{m,h}^{exp}.E_{m,h}^{exp} = \lambda_{m,h}^{imp}.E_{m,h}^{imp} + \gamma_h^{dch} \times \sum_{j=1}^{BES}E_{j,h}^{BES,dch} + \sum_{k=1}^{PV}E_{k,h}^{PV} + \sum_{i=1}^{CGU}E_{i,h}^{CGU} \quad (23)$$

$$E_h^{Load} = E_h^{flex} + E_h^{inflex} \quad (24)$$

Where E_h^{Load} represents the total load demand of the microgrid, comprising both the flexible portion E_h^{flex} and the critical portion E_h^{inflex}. To prevent the EMS from engaging in opportunistic behaviour, such as importing electricity at a time step and then exporting it for profit at the next time step:

$$\varphi_{m,h}^{exp} \le \varphi_{m,h}^{imp} \forall m \in M \quad (25)$$

To avoid buying and selling at the same time:

$$\lambda_{m,h}^{imp} + \lambda_{m,h}^{exp} = 1 \forall m \in M \quad (26)$$

where $\lambda_{m,h}^{imp}$, $\lambda_{m,h}^{exp}$, $\gamma_{j,h}^{ch}$, $\gamma_{j,h}^{dch}$ $\epsilon\{0,1\}\forall(m \in M, j \in J)$.

3.2. The upper layer: sustainable decision-making for the optimal solution

Following the optimization of individual microgrids, the second layer of energy management is geared towards holistic optimization with a sustainable consideration. The centralized C-EMS achieves economic optimization by giving preference to local renewable-based sources to fulfil total demand, thereby minimizing reliance on grid purchases or conventional generation units and subsequently reducing CO2 emissions. Therefore, this phase involves prioritizing economic gains, mitigating CO2 equivalent emissions, and supporting customer welfare. Furthermore, regarding customer welfare, C-EMS solutions prioritize meeting all demand, even if it necessitates purchasing from the grid, ensuring efficient, environmentally conscious, and reliable daily operational strategies for SBES and transactions within the system and with the grid. The concept here is to refrain from shedding any loads unless the cost of meeting the demand surpasses a predefined threshold determined by the system operator, while also taking into account that

incentives should be paid to consumers who offer flexibility.

- Optimization Problem Formulation

This phase of optimization produces the optimal solution for the entire cluster. As denoted by **Eq. (27)**, the formulation of the system to be optimized deviates slightly from that of the lower level. In this context, constraints require revision, particularly the power balance constraint. Additionally, the formulation of the objective function needs updating, as the proposed strategy does not consider any generation from the community, unlike for individual microgrids.

$$OF-II: min \sum_{h=1}^{H} \left\{ \left(Cost_{C-EMS}^{exchange} + Cost_{C-EMS}^{SBES} + Cost_{C-EMS}^{flex} \right\} \right. \tag{27}$$

In eq. (27), the first term represents the expenses associated with grid exchanges by the C-EMS, the second term covers the cost of SBES operation, and the third term reflects the expenditure required to compensate consumers for providing flexibility. In the second layer, the generation deficiencies of microgrids and their available excess generations serve as the demand (L_h^{C-EMS}) and energy source (G_h^{C-EMS}) for C-EMS. Eqs. (28) to (29) describe how to calculate these parameters based on the optimal operational schedules of microgrids.

$$D = G_h^{C-EMS} - L_h^{C-EMS} \tag{28}$$

$$\begin{bmatrix} d_{1,1} & \cdots & d_{1,h} \\ \vdots & \ddots & \vdots \\ d_{m,1} & \cdots & d_{m,h} \end{bmatrix} = \begin{bmatrix} g_{1,1} & \cdots & g_{1,h} \\ \vdots & \ddots & \vdots \\ g_{m,1} & \cdots & g_{m,h} \end{bmatrix} - \begin{bmatrix} l_{1,1} & \cdots & l_{1,h} \\ \vdots & \ddots & \vdots \\ l_{m,1} & \cdots & l_{m,h} \end{bmatrix} \tag{29}$$

Where D shows the deviation. Let x_h equal to $\sum_{m=1}^{MG} D_{m,h} \forall_h$ then

$$G_h^{C-EMS} = \begin{cases} |x_h| \; if \;\; x < 0 \\ 0 \;\; otherwise \end{cases} \tag{30}$$

$$L_h^{C-EMS} = \begin{cases} x_h \; if \;\; x > 0 \\ 0 \;\; otherwise \end{cases} \tag{31}$$

- The SBES model

In the second layer of energy management, the same mathematical formulation for storage systems detailed in Eqs. (10) to (20) is utilized, albeit with minor adjustments. In addition to accounting for degradation costs and the expense related to CiOS, it is crucial to consider the investment cost associated with installing SBES. Investment costs are accounted for only in the upper layer, as this layer is responsible for clustering and managing shared resources like SBES, which require new expenditures. In contrast, the lower layer focuses on optimizing the operational schedules of existing microgrids, without considering additional investment costs, since it operates within the framework of current assets. Given that larger BESs typically employ lead-acid technology [23], **Eq. (32)** calculates the daily life or investment cost of SBES, while ϕ denotes the annual cost of SBES per unit capacity and Cap_{max}^{SBES} represents the SBES's maximum capacity. As obvious, it does not depend on the operating energy flow of SBES.

$$Cost_{life}^{SBES} = \phi . \left(\frac{Cap_{\max}^{SBES}}{365} \right) \tag{32}$$

The integration of BES aims to mitigate fluctuations in renewable energy generation and enhance system reliability. Despite the efforts of energy management systems to find optimal solutions, there remains a risk of some loads going unsupplied due to inaccuracies in load demand and renewable generation forecasts. To mitigate this risk, a spinning reserve is essential, ensuring adequate backup power is available to meet unexpected demand fluctuations. Therefore, the objective at this level shifts towards achieving sustainable solutions, wherein the minimum spinning reserve is factored in. This reserve constitutes the unused portion of the SBES or the residual SoC limit. The determination of this reserve amount is contingent upon the forecast accuracy of historical data, guaranteeing sufficient backup capacity. The equality constraints outlined by Eqs. (33) and (34) fulfil this backup requirement.

$$SoC_{\min}^{SBES} = \alpha_{\min}^{SBES} . Cap_{\max}^{SBES} \tag{33}$$

$$SoC_{\max}^{SBES} = \beta_{\max}^{SBES} . Cap_{\max}^{SBES} \tag{34}$$

Where α_{min}^{SBES} and β_{min}^{SBES} are the coefficients to limit the minimum and maximum of SBES's SoC with regard to its capacity, and: $\alpha_{min}^{SBES}, \beta_{max}^{SBES} \in [0,1], \alpha_{min}^{SBES} < \beta_{max}^{SBES}, \beta_{max}^{SBES} \neq 0$.

- The grid exchange Model for C-EMS

Similar to layer 1, the grid transactions of C-EMS are delineated by the hourly power exchange rate, integrating buying and selling prices with the assistance of binary variables to enable or disable grid exchange, as follows:

$$Cost^{grid} = \sum_{h=1}^{H} \lambda_h^{buy} E_h^{buy} \varphi_h^{buy} - \lambda_h^{sell} E_h^{sell} \varphi_h^{sell} \tag{35}$$

In this equation, E_h^{buy} and E_h^{sell} denote buying and selling electricity to/from the main grid, respectively, while λ_h^{buy} and λ_h^{sell} represent unit prices of buying and selling at hour h, respectively. To limit the quantity of electricity purchased/sold from/to the main grid:

$$\lambda_h^{buy} . E_h^{buy} \leq P_{\max}^{buy} \tag{36}$$

$$\lambda_h^{sell} . E_h^{sell} \leq P_{\max}^{sell} \tag{37}$$

Considering the model of SBES, the minimization problem can be therefore formulated as follows:

OF-II:

$$min \sum_{h=1}^{H} \left\{ \left(\lambda_h^{buy} . E_h^{buy} . \varphi_h^{buy} - \lambda_h^{sell} . E_h^{sell} . \varphi_h^{sell} \right) + \left(\alpha^{SBES} . \left(E_h^{SBES} \right)^2 + \beta^{SBES} \right) + \left(L_{h,app}^{flex} . \varphi_h^{shed} \right) \right\} \tag{38}$$

Where $\lambda_h^{buy}, E_h^{buy}, \lambda_h^{sell}, E_h^{sell}, L_{h,app}^{flex}, E_h^{SBES}, \gamma_h^{ch}, \gamma_h^{dch}$ are the decision variables. It is worth mentioning that the total operational cost of C-EMS includes CiOS. However, since CiOS constitutes a small portion compared to the overall operational cost, it will be factored into the optimal cost at the end for further calculations. This approach helps avoid rendering the problem non-convex.

- The power balance considering demand-side flexibility

The balance between available generation, consumption demand, and grid exchange is guaranteed by Eqs. (39) to (42):

$$L_h^{flex} = \sum_{m=1}^{MG} E_h^{flex} \tag{39}$$

$$L_{h,app}^{flex} = L_h^{flex} - L_{h,unapp}^{flex} \tag{40}$$

$$L_h^{C-EMS} + \gamma_h^{ch} . E_h^{SBES,ch} + \lambda_h^{buy} . E_h^{buy} - L_{h,app}^{flex} = \lambda_h^{sell} . E_h^{sell} + \gamma_h^{dch} . E_h^{SBES,dch} + G_h^{C-EMS} \tag{41}$$

$$0 \leq L_{h,app}^{flex} \leq L_h^{flex} \tag{42}$$

If the system is operating in the islanded mode then the condition in **Eq. (43)** in the optimization problem should be applied.

$$\lambda_h^{sell} = \lambda_h^{buy} = 0 \tag{43}$$

As previously stated, to avoid charging while buying from the grid λ_h^{buy} and λ_h^{ch} can be set to be complementary as denoted by **Eq. (44)**. Nevertheless, it still may go for discharging while selling to the grid.

$$\lambda_h^{buy} + \gamma_h^{ch} = 1 \tag{44}$$

3.3. Data privacy considerations

An effective communication system is essential for the functionality of MC. The extent of communication needed is a crucial factor influenced primarily by the type of control implemented [8]. By transmitting only aggregated information to C-EMS, the proposed strategy effectively reduces the exposure of sensitive data to potential cyber threats and minimizes the risk of disclosing operational details, thereby enhancing the overall security and privacy of the cluster. More specifically, the proposed strategy leverages the disparity between load demand and available generation communicated to C-EMS to limit the data exchange and retain data privacy. Conversely, once the optimal schedules are computed and prepared for transmission to individual microgrids, only limited information regarding each microgrid's exchange balance and the required flexibility for MC optimal operation is sent individually, with this data not being publicly accessible.

Algorithm 1. The pseudo-code of the proposed Strategy

Input: Forecasted load demand, RES gen, Market price, Component's specification
1: Begin
2: Set H (day-ahead)
3: Read the forecasted data of load, irradiance, and market price
4: Formulate the components's cost:
CGU, PV, BES (ch/dch, CiOS), Exchange
5: For each microgrid in MGs set:
6: Create a new Gurobi model
7: Add decision variables to the model:
CGU, PV, and BES Schedule and activation binary variables
8: Set initial values and bounds
9: Set constants parameters (ρ , ξ, α, β)
10: Create a Gurobi linear expression to hold the OF for new components
11: Build the day-ahead OF expression using a summation loop over H
12: Set the objective function as minimization
13: Add constraints
Power balance, BES ch/dch, PV gen. limit,
CGU gen., limits and ramp rates, number of CiOS
14: Optimize the MIQP model
15: Store optimized values in arrays for further calculation
16: Calculate the cost associated with components (i.g. CiOS)
17: Clear the Gurobi model to define a model for the next in MGs set
18: End for

19: Calculate the MC's excess gen. and deficiencies
20: Trade-off between neighbouring microgrids
21: Calculate the D, G and L matrices
$x_g=|x|$ *if* $x<0$ *otherwise* $x_g=0$
$x_l=x$ *if* $x>0$ *otherwise* $x_l=0$
22: Initialize SBES:
23: Set SoC^{max} and SoC^{min}
24: Get max quantity and incentive of flexibility
25: Create a new MIQP Gurobi model:
26: Execute steps (7) to (15) for the current model
27: Send optimized schedules to MGs
28: End
Output: Optimized MC schedules and flexibility

3.4. Solving the optimization problem

Researchers explore various techniques for solving energy management optimization problems in microgrid applications, including neural networks and machine learning methods [24–26], game theory [25,27], and multi-agent systems [28,29]. However, these approaches face challenges such as reliability issues, avoiding local minima traps, and computational efficiency concerns, particularly in managing energy storage operations. Therefore, some researchers have opted to employ linear and non-linear mathematical programming [26,29], because of the exactness of such methods. Hence, in this paper, precise mathematical formulations are proposed, employing mixed-integer quadratic programming (MIQP) to accurately determine optimal solutions for generation scheduling and exchanges. It is worth noting that converting nonlinear terms into linear forms facilitates reformulating the problem as mixed-integer linear programming (MILP), aiming to improve computational efficiency, albeit with some estimation involved. Therefore, in addressing both accuracy and computational resource concerns, this paper utilizes Mixed-Integer Quadratic Programming (MIQP), solved using the Gurobi™ optimizer in Python, to attain the day-ahead optimal schedule for the cluster. The proposed optimization procedure is outlined in **Algorithm (1)**.

4. Results and discussion

In this section, several experiments and case studies are conducted to evaluate the effectiveness of the proposed two-layer energy management, utilizing real data from a cluster of three microgrids and price data obtained from the Australian energy market for the NSW state.

4.1. System initialization

The system schematic is shown in Fig. 5, where three microgrids, each with CGUs, PVs, BESs, and both flexible and critical load demands, are clustered in an MPSC configuration with SBES. As outlined in Section 1, in this configuration energy can flow between each microgrid and also to and from the main grid. Each microgrid in the cluster is equipped with identical types of components—PVs, BESs, and CGUs—in terms of type, technology, and model coefficients, though their sizes differ. The capacities of the CGUs (natural gas generators) and BESs for the three microgrids are set at 40 kW, 50 kW, and 70 kW, and 71 kWh, 28.4 kWh, and 56.8 kWh, respectively. A sensitivity analysis is conducted for the SBES capacity. A central energy management system optimizes the operation of these microgrids over a day-ahead timeframe, divided into 24 timeslots. Initial parameter values are provided in Table 1 for reference, with uniform characteristics assumed across all microgrids for simplicity. The calculation of load flexibility considers the collective flexible and inflexible load demands of microgrids.

Fig. 6 illustrates the input values representing the buying and selling prices from/to the main grid. To prevent the EMS model from repeatedly buying energy in one hour and selling it in the next, the selling price is deliberately set lower than the buying price. This pricing strategy discourages opportunistic behaviour by ensuring that the cost of purchasing energy is always higher than the revenue from selling it which is the current policy in Australia, thereby promoting optimal system operation and ensuring stable market conditions. As shown, the price starts low at the beginning of the period, undergoes fluctuations until hour 16, spikes at hour 17, and subsequently decreases to approximately $0.37 and $0.33 per kilowatt-hour for importing and exporting energy, respectively. Transactions, i.e. buying and selling, within the microgrid cluster are considered to occur at the same price level as transactions with the main grid. This approach ensures consistency and aligns with market dynamics. When the selling or buying price within the system is lower than the market price, microgrids are incentivized to procure electricity directly from the grid rather than from neighbouring microgrids. Conversely, if the selling or buying price exceeds the market rate, microgrids are encouraged to supply power directly to the grid instead of collaborating with other microgrids. This strategy optimizes cost-effectiveness and operational efficiency within the cluster of microgrids.

The solar irradiance in the region where the microgrid cluster is located, along with the characteristics and efficiency of the PV units, is

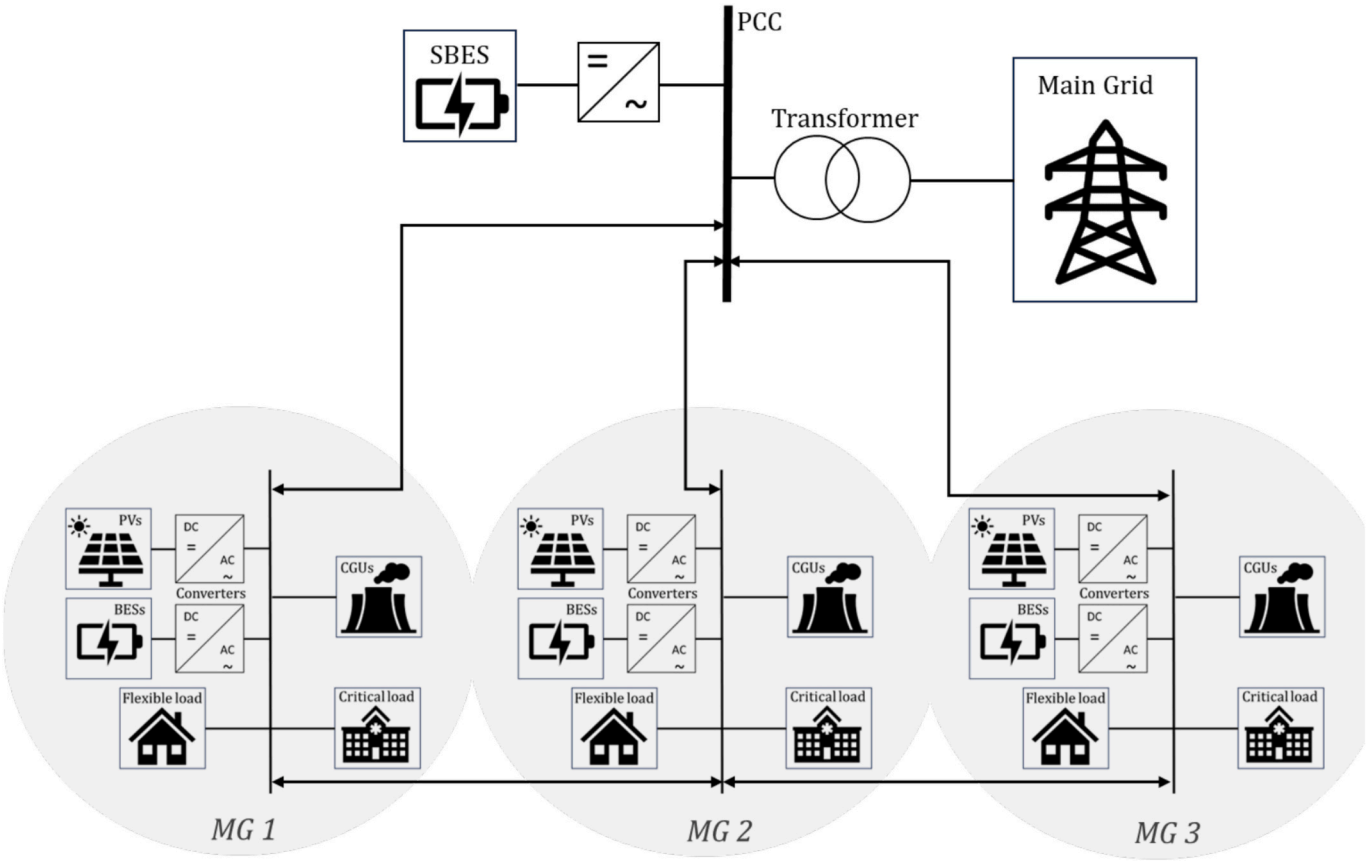

Fig. 5. Schematic representation of the grid-connected microgrid cluster as the case study.

Table 1
Component's input parameters.

Parameter	*Value*
$a_i^{CGU}, b_i^{CGU}, c_i^{CGU}$	*0.00332, 0.06, 2.5*
R_m^{CGU}	*(10,20,20)*
$\alpha_j^{BES}, \beta_j^{BES}$	*0.00108, 0.5*
$\alpha_{j,min}^{BES}$	*0.05*
$\beta_{j,max}^{BES}$	*1*
ξ	*10*
ρ_j	*0.23*
σ_k	*0.005*

utilized to calculate the output generation of PVs within each individual microgrid illustrated in Fig. 7. It is notable that microgrid 3 exhibits the highest renewable generation capacity among the three microgrids, while microgrid 2 demonstrates the lowest applicable capacity. Fig. 8 showcases the initial load demand profiles of individual microgrids. Microgrid 1 depicts a peak demand of 62 kW around hour 21, while microgrid 2 peaks at 83 kW during the morning hours around hour 10. On the other hand, microgrid 3 consistently demonstrates higher demand compared to the other two microgrids, with a peak of 129 kW occurring around hour 21. Additionally, microgrid 3 experiences peaks at hours 12 and 15. These variations in load demand significantly impact the scheduling of generation and the operation of BESs within the EMS, necessitating the utilization of available resources to meet the demand fluctuations.

Figs. 9 and 10 depict the flexibility price and the demand-side flexibility provision at each hour. In cases where flexibility is applied and certain loads are shed, the system operator is required to compensate the affected consumers accordingly.

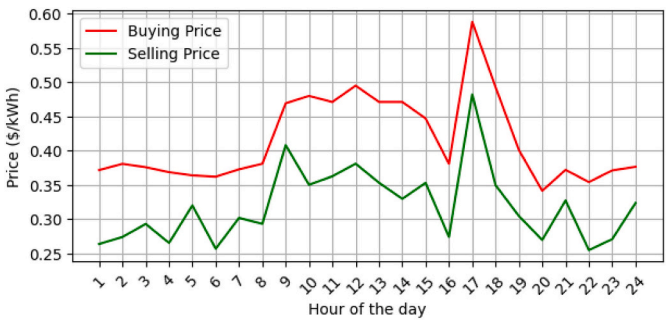

Fig. 6. Buying and selling price from/to the main grid.

4.2. *Conventional energy management approach as the benchmark (layer one)*

Operating individually, microgrids often face challenges in meeting their load demands throughout various time intervals. As depicted in Fig. 11, during peak demand periods, microgrids experience severe negative imbalances, while during load demand profile valleys, positive imbalances indicate surplus generation available for trading, either with neighbouring microgrids or the main grid. Specifically, microgrid 3 encounters negative imbalances in power and demand except for some hours of the period (hours 10 to 13). Microgrid 2 also experiences a comparable situation. Conversely, microgrid 1 witnesses a more balanced situation with having negative generation-consumption balance in the period between 14 and 24 and requiring energy imports.

The optimized generation and consumption profiles of each microgrid within the cluster are presented in Figs. 12(a) to (c), where the

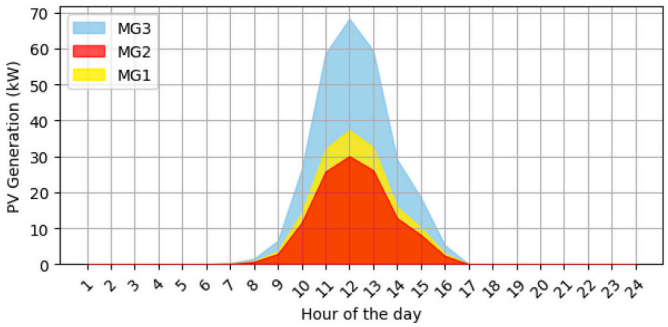

Fig. 7. PV generation output of microgrids within the cluster.

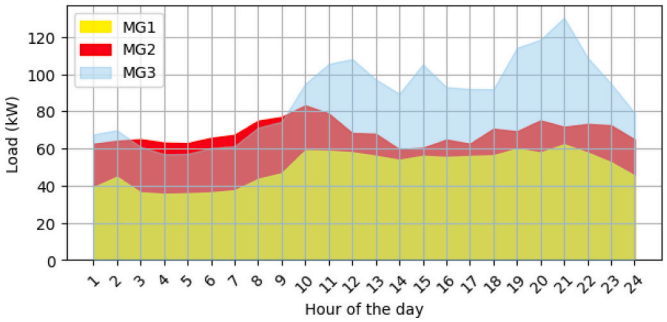

Fig. 8. Initial load demand of microgrids.

required power for import and the total available power, inclusive of generation and battery discharging within the microgrid, are compared to the total demand, encompassing consumer load and battery charging, as well as the initial load demand. This analysis reveals instances where the microgrid's BES demands power for import from external sources, as well as occasions where the BES contributes to meeting demand, reducing the required import power compared to the available generation within the grid. For instance, during the period from hours 1 to 8, microgrid 1 experiences a scenario where the load remains mostly below the generated power, yet the total required power is elevated due to BES charging during intervals of lower market prices, intended for discharge during high-price intervals. Conversely, for hours 9 and 10, when prices are high, EMS discharges the BES, aligning the total available power with the total required power and the initial load. However, a spike in price at hour 17 prompts the EMS to charge the BES beforehand at hours 11 to 13 for discharge. In addition, at hour 12 the excess generation is sold to the grid. At hour 17 the total available power is much more than both initial load and required power, resulting in selling electricity to the grid to make a profit. The situation changed during the remaining hours due to the EMS's decision to import electricity from external sources at hours 19 to 24.

The same analysis can be applied to microgrids 2 and 3. To regulate trading with the grid, while importing and/or exporting, the binary variables $\lambda_{m,h}^{imp}$, $\lambda_{m,h}^{exp}$ can be assigned a value of zero. In such a scenario, the load demand must be met either by internal sources or, in the worst-case scenario, it may remain unmet.

Figs. 13 and 14 showcase the unsupplied demand for microgrids and their available excess generation for export. The EMSs strive to minimize the operational costs of individual microgrids by optimizing the coordination of BESs charging and discharging, as well as the import or export of electricity, considering load demand flexibility. As a result, there are occasions when generated power is available for export, while at other times, power must be imported to fulfil critical demands. Fig. 15 displays the CiOS for each microgrid's BES alongside their power profiles. CiOS increments by one whenever the BES's power profile intersects the zero line. Consequently, as long as the profile remains above or below the zero line, the CiOS is not involved in the BES's costs. Therefore, fluctuations in power quantity do not affect CiOS, although they do influence the total degradation cost slightly. Additionally, Fig. 16 reveals that changes in the SoC of BESs generally follow a similar pattern due to identical market prices faced by all EMSs. However, SoC changes are influenced by the initial SoC value and BES capacity. Notably, the diverse decisions made for different microgrids result in varying SoC changes across different time intervals.

The computation of operational costs for individually operating microgrids follows the methodology detailed in section 3. Fig. 17 offers an analysis of these costs across the microgrids within the cluster. Specifically, the day-ahead operational costs for microgrids 1, 2, and 3 amount to $288.5, $463.67, and $580.04, respectively. Therefore the total operation cost when the energy management is performed in only

Fig. 9. Flexibility price (payable by the operator to consumers).

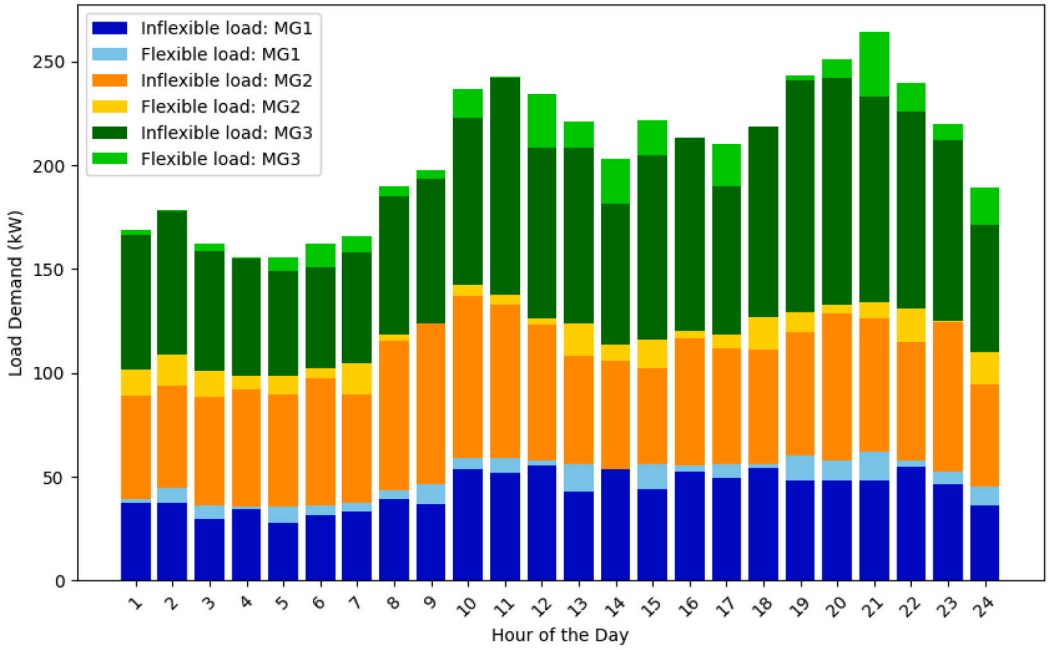

Fig. 10. The total flexible and inflexible load demand of microgrids.

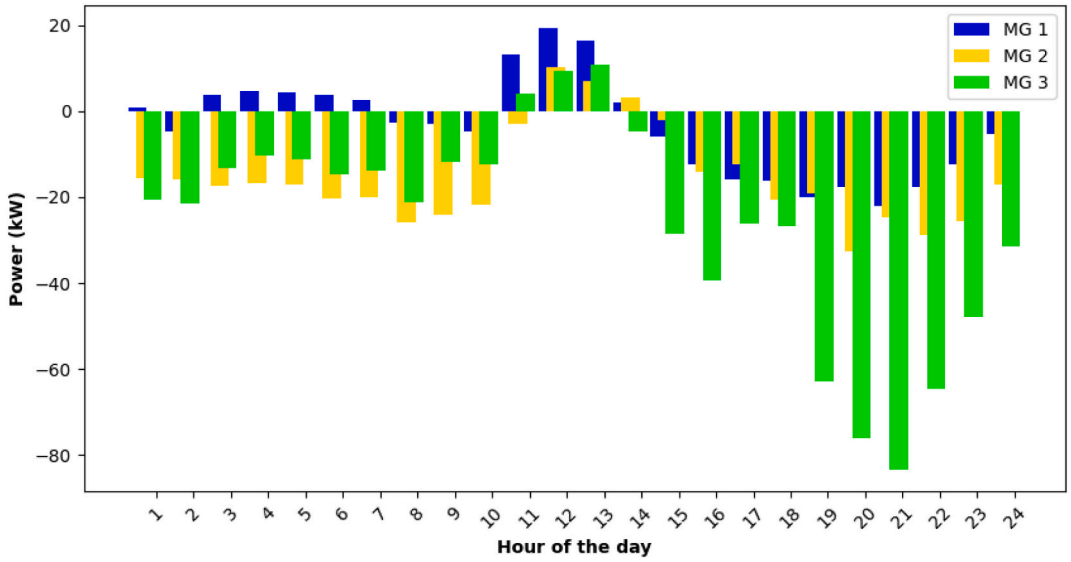

Fig. 11. Total generation and demand imbalance of microgrids in individual operation mode.

one layer would be 1332.21. Notably, the depicted data reveals a proportional correlation between operational costs and the respective load demand levels of each microgrid.

4.3. Performance evaluation of the proposed two-layer strategy with sensitivity analysis

When incorporating the SBES in the C-EMS framework, a distinct analytical approach is necessary. The primary scenario, or base case (BC), for the upper-layer energy management, involves an initial SoC set at 10 %, SBES capacity at 60 kWh, and fluctuating load demand. Under these conditions, the SBES operating state undergoes 15 changes, incurring an associated cost of $3.45. The percentage of cost attributed to CiOS stands at 1.14 %. Consequently, the total operational cost of SBES reaches $7.614, contributing to the overall operational cost of C-EMS amounting to $300.205. Furthermore, the total system operational cost, encompassing exchanges and microgrid internal costs, sums up to $1239.543. The total cost of the conventional energy management approach, calculated in the previous subsection, tallies $1332.206 for individual operations. Based on this value with the current SBES configuration, the overall cost reduction occurred in the upper layer for the entire system accounts for $92.66, representing a 6.96 % decrease, compared to one-layer energy management. Fig. 18 elucidates the performance of C-EMS in determining whether to buy or sell electricity or to charge or discharge SBES. At hour 17, the optimal decision is to sell electricity to the main grid while simultaneously discharging SBES. The stored energy in SBES charged from hours 10 to 15, combined with local generation, adequately meets the load demand in subsequent hours, allowing surplus energy to be sold to the grid for profit, given the higher price during those timeslots. Fig. 19 delineates the operating state and

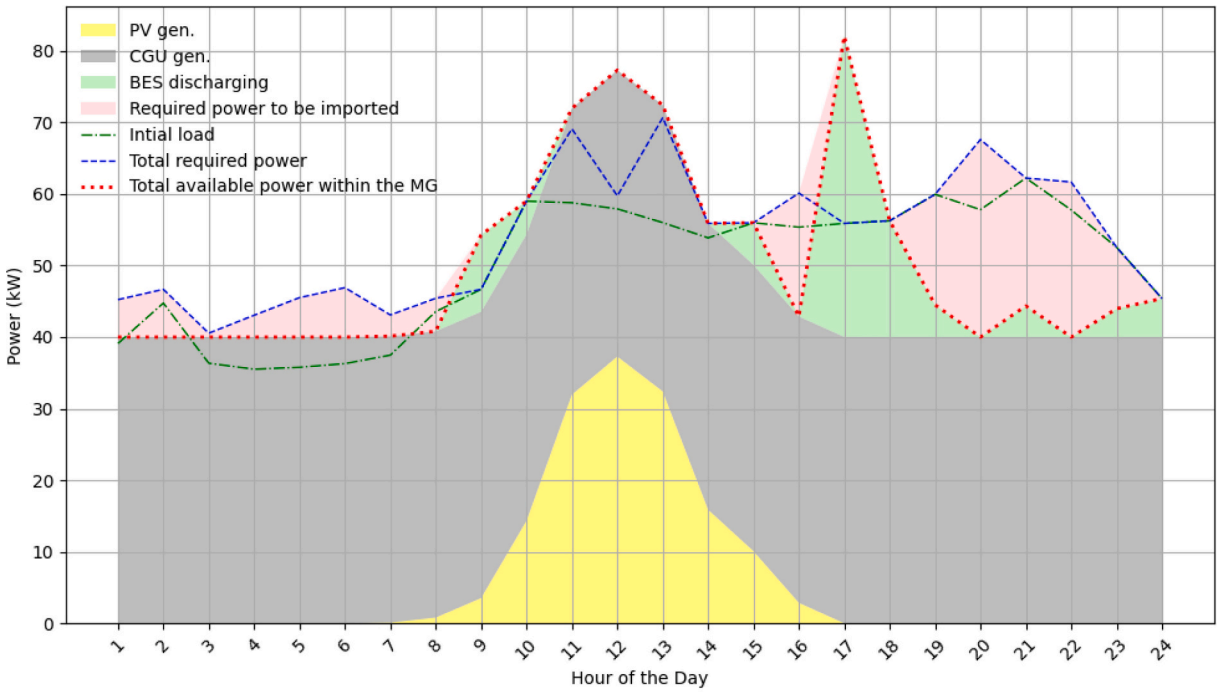

(a)

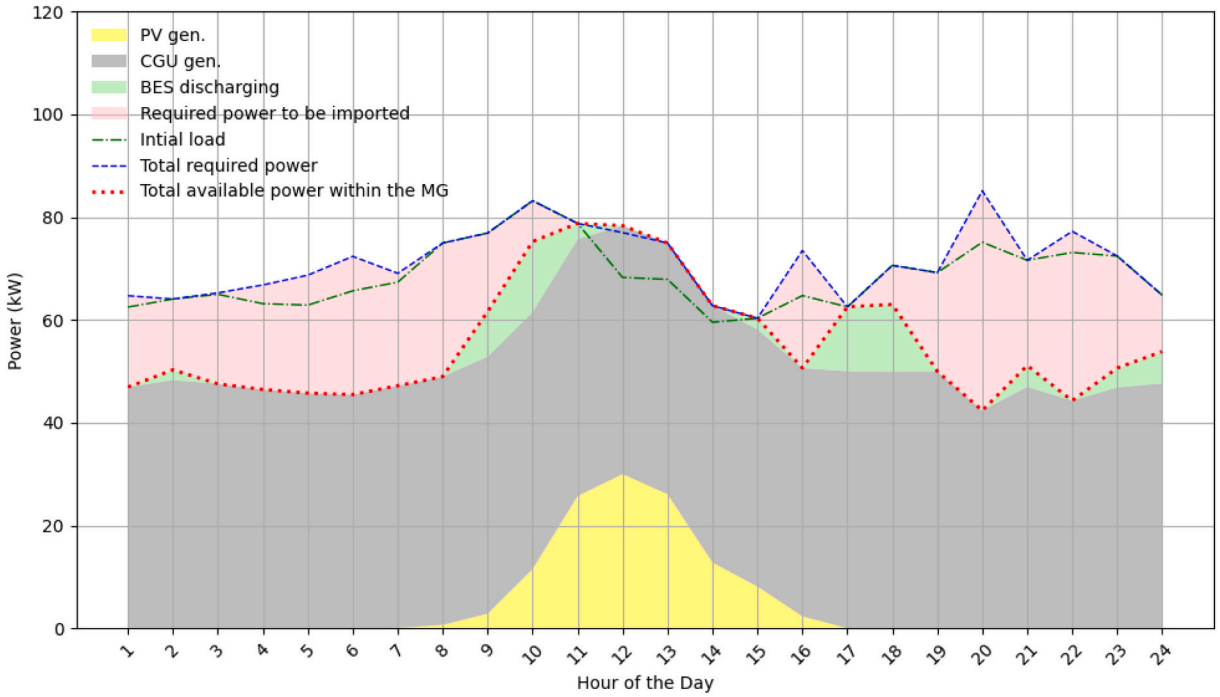

(b)

Fig. 12. (a) Generation and consumption levels of microgrid 1. (b) Generation and consumption levels of microgrid 2. (c) Generation and consumption levels of microgrid 3.

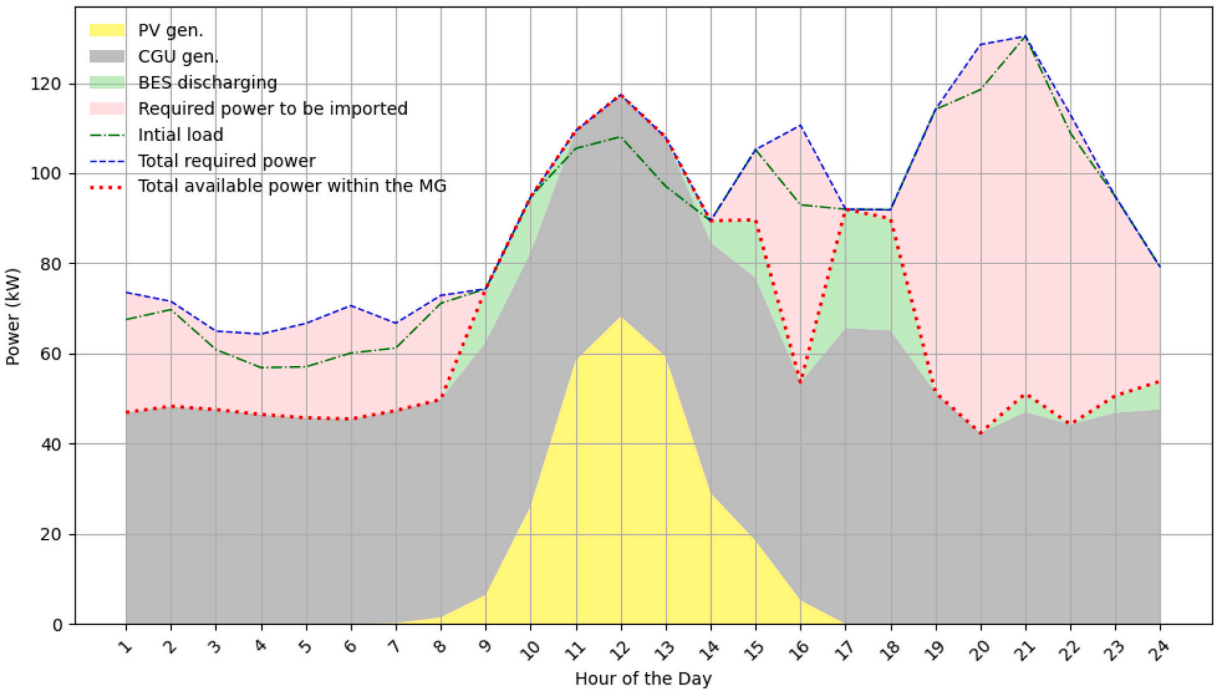

(c)

. (*continued*).

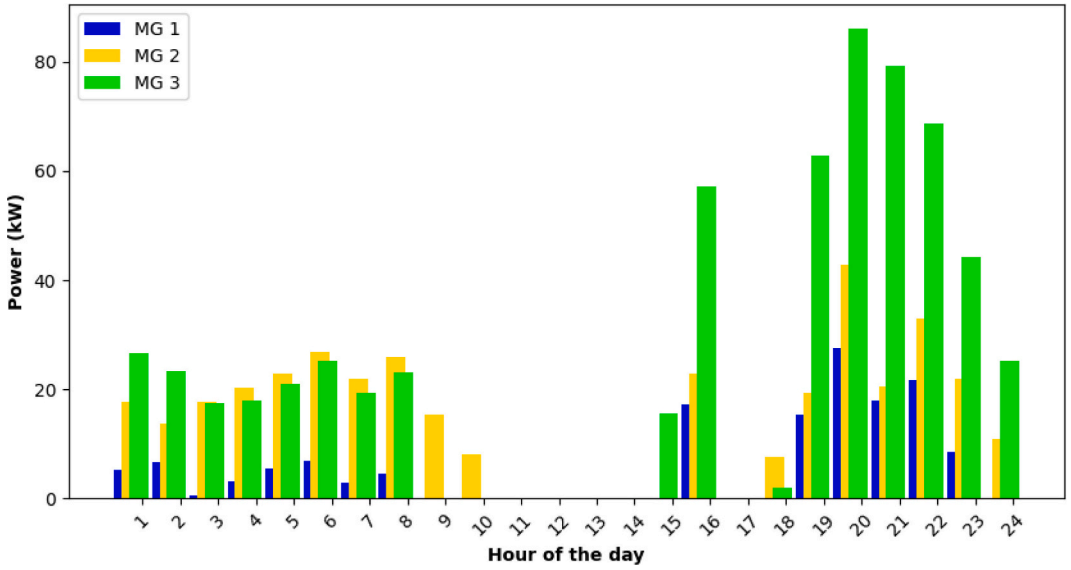

Fig. 13. Required power to be imported by each microgrid (unsupplied demand).

SoC of the SBES, illustrating a pattern where the battery undergoes charging primarily during initial intervals to meet the required energy demand at hour 10. Subsequently, the charging pattern continues until hour 16 to facilitate discharge during the peak market price at hour 17, reaching a fully discharged state by hour 24.

Various constants and coefficients of components, alongside variables such as demand and price, significantly influence the optimal solution derived by C-EMS. These factors encompass the capacity, initial SoC, cost coefficients of the SBES, and the price applied for load flexibility. For instance, when the flexibility price surpasses the buying price from the grid, C-EMS opts not to utilize any flexibility. To examine the impact of these variables, Table 2 delves into the sensitivity of optimal decisions and the corresponding operational costs in response to changes in the flexibility price from the consumer side. As outlined in this table, for flexibility prices marginally below the buying price, some portions of flexibility are applied throughout the timeframe; however, this is not the case in real systems. In the base case scenario as a realistic one, nearly 93 % of available flexibility is deemed applicable. Fig. 20 illustrates this hourly, demonstrating that only during hours 14 and 15 when the market price approximately aligns with the flexibility price, a portion of flexibility is not applied. In scenarios where the operator can shed loads at no cost (experiment 7), the entire portion of available flexibility is decided to be shed. Additionally, Table 3 presents a sensitivity analysis of the optimal solution, focusing on the total system cost

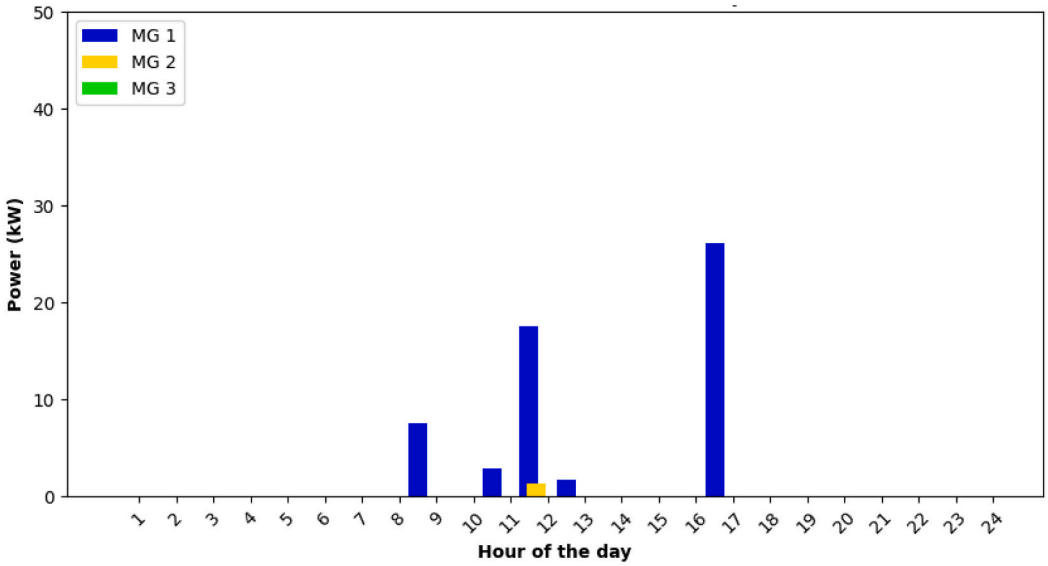

Fig. 14. Available excess generation of each microgrid.

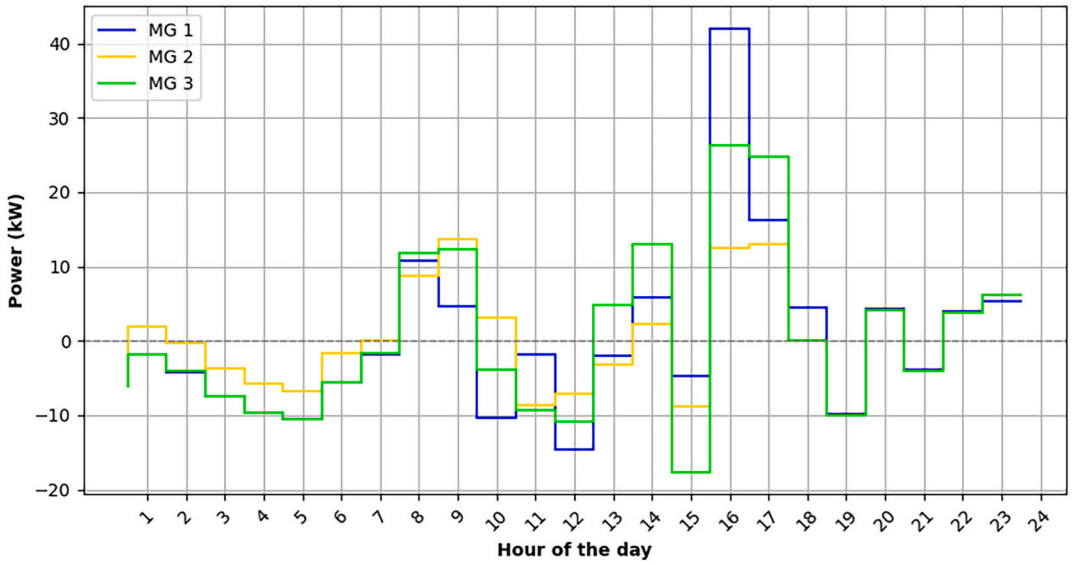

Fig. 15. Individual microgrid's BES day-ahead operation profile.

and the costs associated with SBES operation in relation to the SBES initial SoC and installed capacity. The table ranges the SBES capacity from 20 to 80 kWh, while the remaining charge varies from 0 to 50 kW, allowing for a comprehensive assessment of their effects on other dependent variables. The analysis reveals a range of total cost reductions from 6.5 % at the minimum to 8.1 % at the maximum, depending on these parameters. Even in scenarios where no flexibility is available and the demand is deemed entirely uninterruptible, C-EMS still observes a reduction in operational costs, amounting to 1.17 %.

To evaluate the hourly operational costs and emissions of the proposed strategy compared to the benchmark, Figs. 21 and 22 display the hourly costs and emissions across four distinct scenarios. These scenarios encompass the benchmark and base case scenarios, as well as the best setting and maximum flexibility scenarios. The best setting entails an SBES capacity of 80 kWh and an initial remaining charge of 50 kWh. In addition, the maximum flexibility scenario occurs when the operator incurs no cost when utilizing flexibility, resulting in the application of all available flexibility. Fig. 21 illustrates that the hourly operational costs of the base case and best SBES setting scenarios consistently remain below those of the benchmark, with only minor deviations above the benchmark observed at hours 10 and 14. Despite these slight increases, the total operational costs of these scenarios remain lower than the benchmark scenario.

Turning to hourly CO2 equivalent (CO2e) emissions depicted in Fig. 22, it is evident that emissions remain below the benchmark across all scenarios throughout the day-ahead hours. However, there is relatively little variation in emissions for the base case, best SBES setting, and maximum flexibility scenarios. This stability in emissions is attributed to the varying mixture of supplied electricity, whether imported or generated, each contributing to CO2e emissions based on the emission factors of local fossil fuel-based generation and the electricity grid. The emission factor related to any electricity purchased from the Australian electricity grid in NSW state for 2024 is projected to be 0.59 kg/kWh [30,31]. Moreover, the emission factor for CGUs considered in this paper is 0.43 kg/kWh [32]. Overall, the proposed strategy significantly diminishes emissions over the scheduling period, as evidenced.

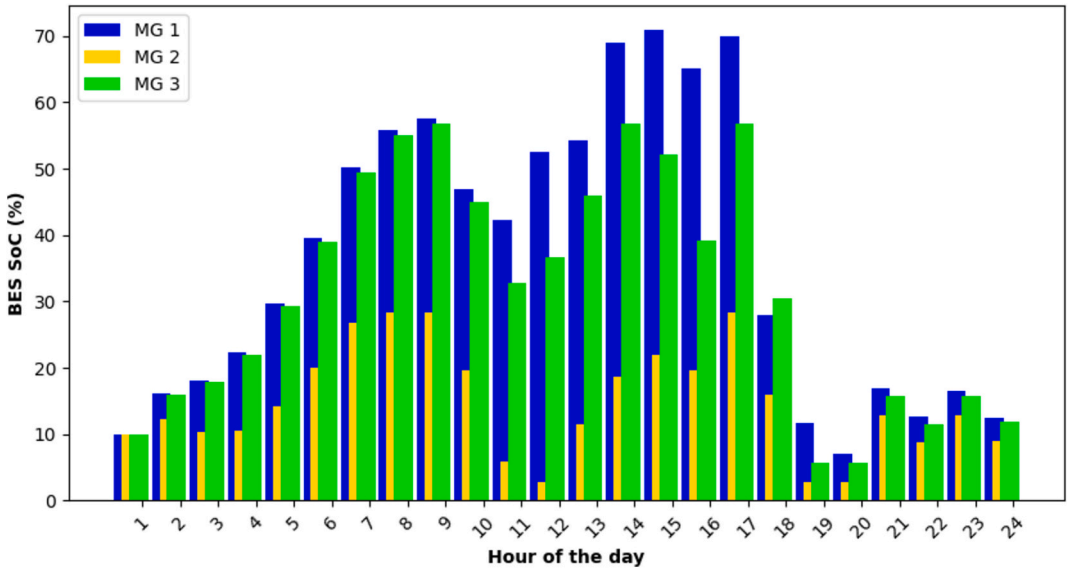

Fig. 16. Individual microgrid's BES SoCs.

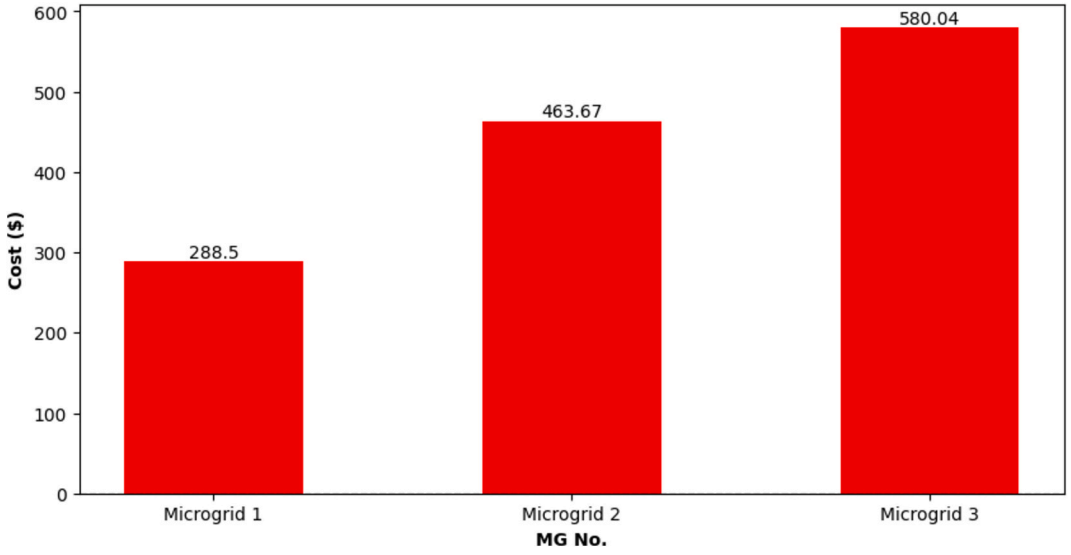

Fig. 17. Individual microgrid's day-ahead operational cost.

Specifically, in the best-setting scenario, there is an impressive 11.6 % reduction in total CO2e emissions compared to the benchmark.

5. Conclusion

The proposed scheduling model seeks to optimize the operational costs of microgrid clusters by integrating an embedded energy storage system, fostering cooperation among microgrids, and facilitating their transactions with neighbouring microgrids or the SBES. Leveraging load/generation disparity information, C-EMS ensures efficient financial exchange and maintains data privacy during data exchange. The mathematical model includes renewable and conventional resources for generation, and particularly for the SBES, incorporates various factors such as charging/discharging costs, cycling costs, and lifespan expenses. It is essential to recognize that the SBES serves as a communal asset, thus requiring the community to provide compensation for both its operational and installation costs. Notably, this strategy not only avoids additional costs but also reduces operational expenses even in the worst scenario while enhancing the flexibility and reliability of the power supply and reducing CO2e emission. By enabling net-zero decisions, operators can also forego purchasing electricity from the main grid, compensating consumers for load shedding to enhance satisfaction and welfare while reducing emissions. However, the strategy is primarily designed for grid-connected microgrids, which restricts its applicability to fully isolated or off-grid microgrids that would require additional operational strategies. The model's performance is also dependent on accurate forecasts of renewable generation and demand, with forecasting errors potentially leading to suboptimal outcomes. Furthermore, the MIQP approach may encounter scalability challenges when applied to more complex systems. Future research could explore profit distribution models for SBES ownership and address the scalability of the optimization framework, as well as potential applications in off-grid systems.

CRediT authorship contribution statement

Farid Moazzen: Writing – original draft, Visualization, Methodology, Formal analysis, Data curation, Conceptualization. **M.J. Hossain:**

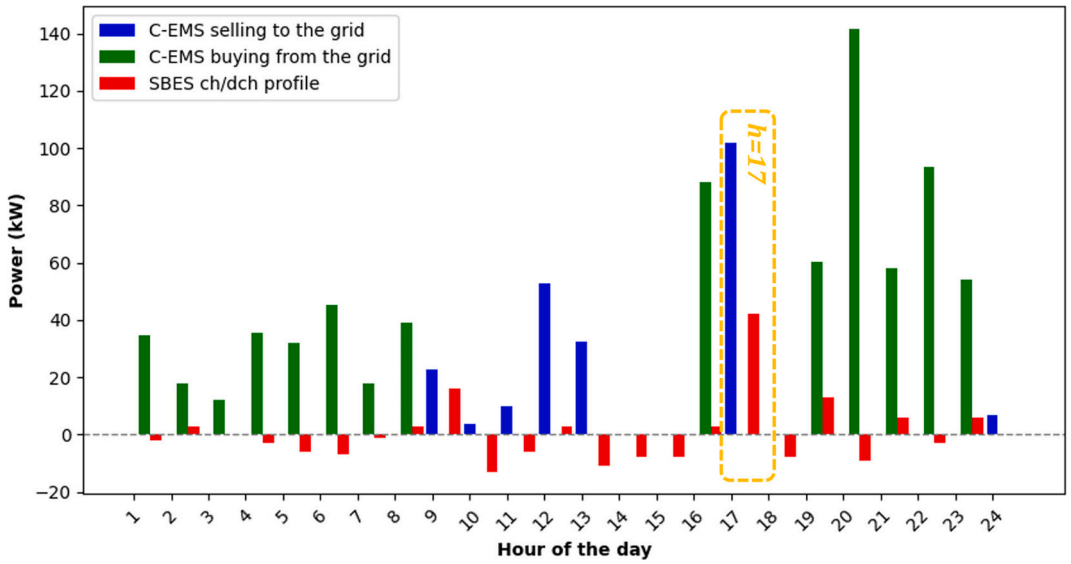

Fig. 18. Optimized energy scheduling profile of the cluster.

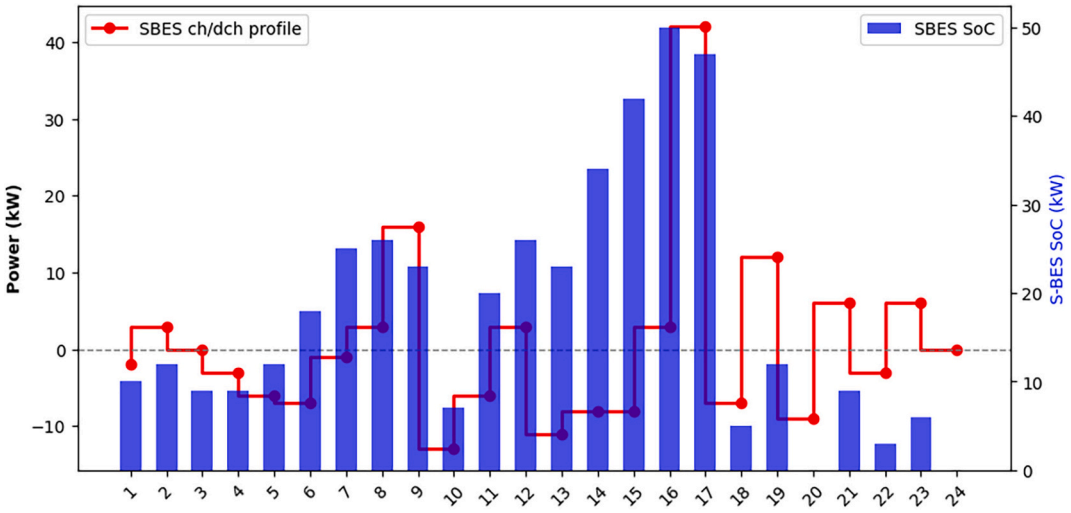

Fig. 19. Optimized SBES ch/dch profile and SoC.

Table 2
The sensitivity of operational costs to $\varphi^{shed.}$

No. of exp.	φ^{shed}	*Total flexibility offered (kWh)*	*Applied flexibility (kWh)*	*Unapplied flexibility (kWh)*	*The cost associated with flexibility($)*	*The total operational cost($)*	*Total cost reduction (%)*
1	$=\sim\varphi^{buy}$	602.12	344.903	257.217	125.433	1328.454	0.28
2	$\varphi^{sell}<\varphi^{shed}<\varphi^{buy}$	602.12	213.549	388.571	74.024	1321.086	0.83
3	φ^{sell}	602.12	465.902	136.218	142.702	1301.945	2.27
4	*BC/2*	602.12	602.12	0	67.37	1172.52	11.98
5	*BC*	602.12	561.25	40.86	120.037	1239.543	6.96
6	*2.BC*	602.12	235.125	366.995	56.43	1301.133	2.33
7	*0*	602.12	602.12	0	0	1105.14	17.04

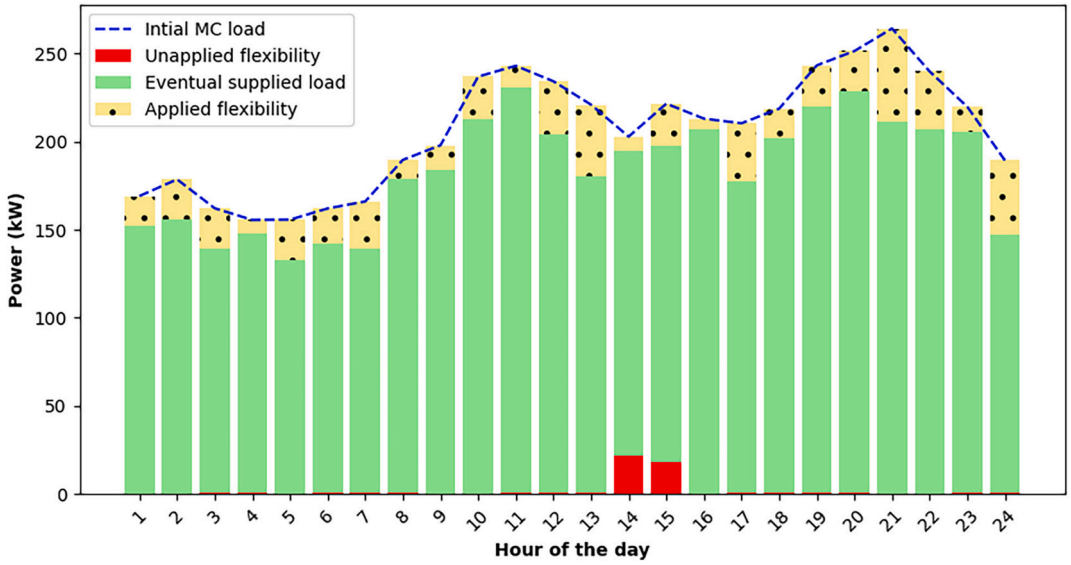

Fig. 20. Supplied load and optimized flexibility applied.

Table 3
The sensitivity of the cluster's total operational cost to SBES capacity and initial SoC

No. of exp.	SBES Capacity (kWh)	Initial SoC* Capacity (kWh)	Number of CiOS	The cost associated with CiOS($)	The cost associated with CiOS(%)	The total cost of SBES operation($)	The total operational cost ($)	The total cost reduction($)	Total cost reduction(%)
1	80	50	15	3.45	1.21	8.844	1224.445	107.761	8.1
2	80	10	15	3.45	1.15	8.726	1239.427	92.779	6.96
3	80	0	15	3.45	1.14	8.642	1243.199	89.007	6.68
4	60	50	14	3.22	1.13	7.362	1224.387	107.819	8.09
5	60	10	15	3.45	1.15	7.654	1239.543	92.663	6.96
6	60	0	15	3.45	1.14	7.66	1243.303	88.903	6.67
7	40	40	13	2.99	1.04	6.098	1228.443	103.763	7.79
8	40	10	14	3.22	1.07	6.396	1239.836	92.37	6.93
9	40	0	15	3.45	1.14	6.614	1243.815	88.391	6.64
10	20	20	14	3.22	1.08	5.494	1237.114	95.09	7.14
11	20	10	15	3.45	1.15	5.726	1241.061	91.145	6.8
12	20	0	15	3.45	1.13	5.73	1244.805	87.401	6.56
13	60 (inflex.)	50	13	2.99	0.79	6.88	1316.524	15.682	1.177

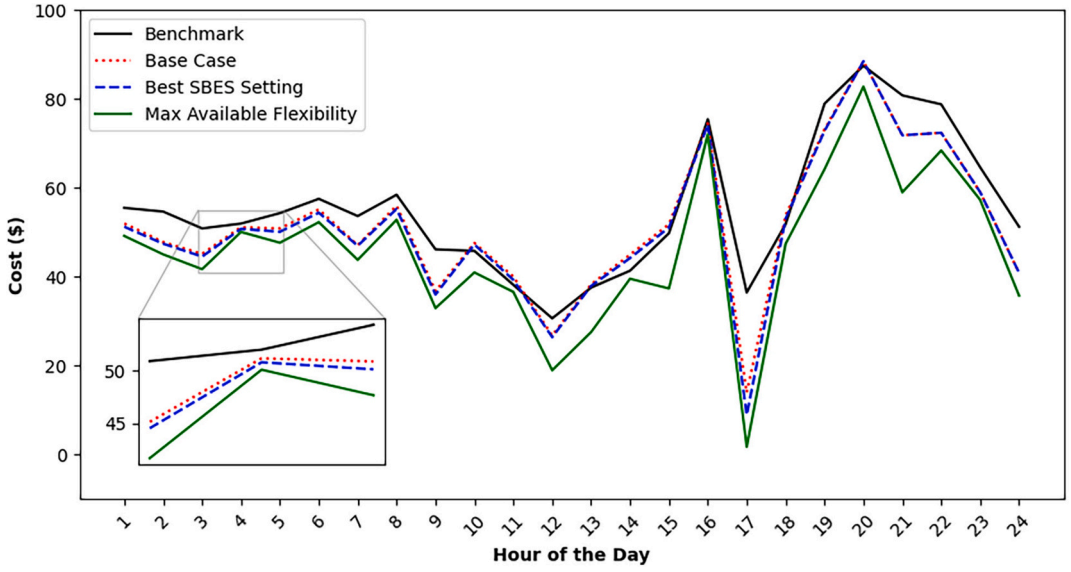

Fig. 21. Hourly operational cost comparison for different scenarios.

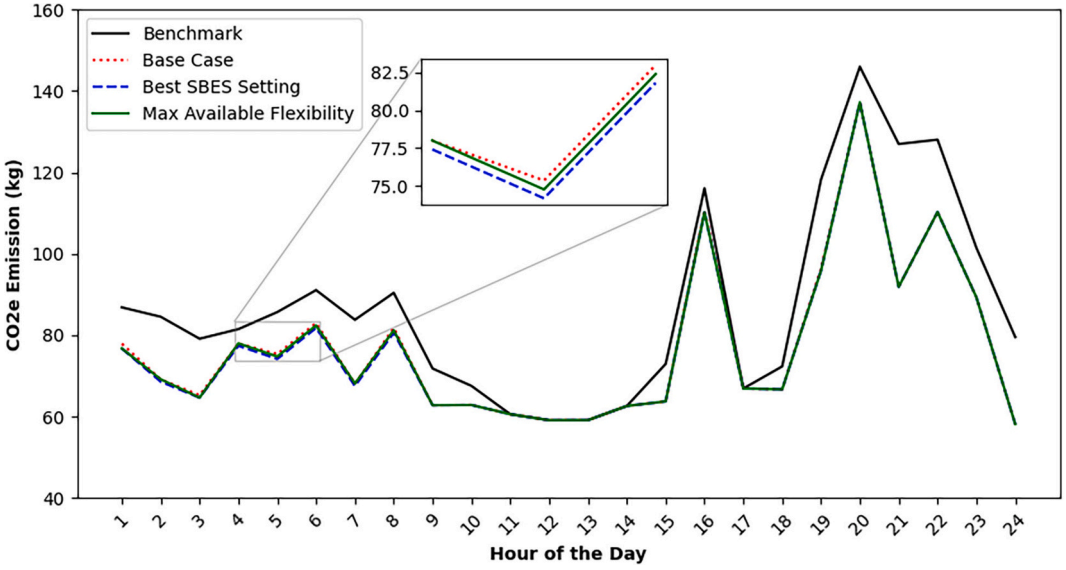

Fig. 22. Hourly CO2e emission comparison for different scenarios.

Validation, Supervision.

Declaration of competing interest

The authors declare that they have no known competing financial interests or personal relationships that could have appeared to influence the work reported in this paper.

Data availability

Data will be made available on request.

References

[1] Mavuri SS, Nakka J, Kotla A. "Interconnected Microgrids: A Review and Future perspectives," in *2022 IEEE 2nd International Conference on Sustainable Energy and Future Electric Transportation (SeFeT)*. 2022. p. 1–7. https://doi.org/10.1109/SeFeT55524.2022.9908988.

[2] Zou H, Mao S, Wang Y, Zhang F, Chen X, Cheng L. A survey of energy management in interconnected multi-microgrids. IEEE Access 2019;7:72158–69. https://doi.org/10.1109/ACCESS.2019.2920008.

[3] Singh AR, Koteswara Raju D, Phani Raghav L, Seshu Kumar R. State-of-the-art review on energy management and control of networked microgrids. Sustain Energy Technol Assess Jun. 2023;57. https://doi.org/10.1016/j.seta.2023.103248.

[4] Fu Y, Zhang Z, Li Z, Mi Y. Energy Management for Hybrid AC/DC distribution system with microgrid clusters using non-cooperative game theory and robust optimization. IEEE Trans Smart Grid 2020;11(2):1510–25. https://doi.org/10.1109/TSG.2019.2939586.

[5] Ma G, Li J, Zhang X-P. A review on optimal energy management of Multimicrogrid system considering uncertainties. IEEE Access 2022;10:77081–98. https://doi.org/10.1109/ACCESS.2022.3192638.

[6] Bandeiras F, Pinheiro E, Gomes M, Coelho P, Fernandes J. Review of the cooperation and operation of microgrid clusters. Renew Sustain Energy Rev 2020;133:110311. https://doi.org/10.1016/j.rser.2020.110311.

[7] Anastasiadis AG, Tsikalakis AG, Hatziargyriou ND. "Operational and environmental benefits due to significant penetration of Microgrids and topology sensitivity," in *IEEE PES General Meeting*. 2010. p. 1–8. https://doi.org/10.1109/PES.2010.5590069.

[8] Bullich-Massagué E, Díaz-González F, Aragüés-Peñalba M, Girbau-Llistuella F, Olivella-Rosell P, Sumper A. Microgrid clustering architectures. Appl Energy 2018;212:340–61. https://doi.org/10.1016/j.apenergy.2017.12.048.

[9] Xu Q, Zhao T, Xu Y, Xu Z, Wang P, Blaabjerg F. A distributed and robust energy management system for networked hybrid AC/DC microgrids. IEEE Trans Smart Grid 2020;11(4):3496–508. https://doi.org/10.1109/TSG.2019.2961737.

[10] Yuan Z-P, Li P, Li Z-L, Xia J. A fully distributed privacy-preserving energy management system for networked microgrid cluster based on homomorphic encryption. IEEE Trans Smart Grid 2023:1. https://doi.org/10.1109/TSG.2023.3309405.

[11] Liu Z, Wang L, Ma L. A Transactive energy framework for coordinated energy management of networked microgrids with Distributionally robust optimization. IEEE Trans Power Syst 2020;35(1):395–404. https://doi.org/10.1109/TPWRS.2019.2933180.

[12] Ceja-Espinosa C, Pirnia M, Cañizares CA. An affine arithmetic-based energy management system for cooperative multi-microgrid networks. IEEE Trans Smart Grid 2023:1. https://doi.org/10.1109/TSG.2023.3306702.

[13] Cui G, Jia Q-S, Guan X. Energy Management of Networked Microgrids with Real-Time Pricing by reinforcement learning. IEEE Trans Smart Grid 2024;15(1):570–80. https://doi.org/10.1109/TSG.2023.3281935.

[14] Yousri D, Farag HEZ, Zeineldin H, El-Saadany EF. Integrated model for optimal energy management and demand response of microgrids considering hybrid hydrogen-battery storage systems. Energ Conver Manage 2023;280:116809. https://doi.org/10.1016/j.enconman.2023.116809.

[15] Xie P, Jia Y, Chen H, Wu J, Cai Z. Mixed-stage energy Management for Decentralized Microgrid Cluster Based on enhanced tube model predictive control. IEEE Trans Smart Grid 2021;12(5):3780–92. https://doi.org/10.1109/TSG.2021.3074910.

[16] Saki R, Kianmehr E, Rokrok E, Doostizadeh M, Khezri R, Shafie-khah M. Interactive multi-level planning for energy management in clustered microgrids considering flexible demands. International Journal of Electrical Power & Energy Systems 2022;138:107978. https://doi.org/10.1016/j.ijepes.2022.107978.

[17] Elmetwaly AH, ElDesouky AA, Omar AI, Attya Saad M. Operation control, energy management, and power quality enhancement for a cluster of isolated microgrids. Ain Shams Eng J 2022;13(5):101737. https://doi.org/10.1016/j.asej.2022.101737.

[18] Wu C, Sui Q, Lin X, Wang Z, Li Z. Scheduling of energy management based on battery logistics in pelagic islanded microgrid clusters. International Journal of Electrical Power & Energy Systems 2021;127:106573. https://doi.org/10.1016/j.ijepes.2020.106573.

[19] Shekari T, Gholami A, Aminifar F. Optimal energy management in multi-carrier microgrids: an MILP approach. Journal of Modern Power Systems and Clean Energy 2019;7(4):876–86. https://doi.org/10.1007/s40565-019-0509-6.

[20] Mohammadpour Shotorbani A, Zeinal-Kheiri S, Chhipi-Shrestha G, Mohammadi-Ivatloo B, Sadiq R, Hewage K. Enhanced real-time scheduling algorithm for energy management in a renewable-integrated microgrid. Appl Energy 2021;304:117658. https://doi.org/10.1016/j.apenergy.2021.117658.

[21] Mohy-Ud-Din G, Vu DH, Muttaqi KM, Sutanto D. "An Integrated Energy Management Approach for the Economic Operation of Industrial Microgrids under Uncertainty of Renewable Energy," in 2019 IEEE Industry Applications Society Annual Meeting. 2019. p. 1–8. https://doi.org/10.1109/IAS.2019.8912399.

[22] Rokh SB, Zhang R, Ravishankar J, Saberi H, Fletcher J. "Real-Time Optimization of Microgrid Energy Management Using Double Deep Q-Network," in 2023 IEEE Power & Energy Society Innovative Smart Grid Technologies Conference (ISGT). IEEE 2023:1–5.

[23] Zhang X, Huang C, Shen J. Energy optimal Management of Microgrid with High Photovoltaic Penetration. IEEE Trans Ind Appl 2023;59(1):128–37. https://doi.org/10.1109/TIA.2022.3208885.

[24] Nakabi TA, Toivanen P. Deep reinforcement learning for energy management in a microgrid with flexible demand. Sustainable Energy, Grids and Networks 2021;25:100413. https://doi.org/10.1016/j.segan.2020.100413.

[25] Samuel O, et al. Towards real-time energy Management of Multi-Microgrid Using a deep convolution neural network and cooperative game approach. IEEE Access 2020;8:161377–95. https://doi.org/10.1109/ACCESS.2020.3021613.

[26] Sharma P, Dutt Mathur H, Mishra P, Bansal RC. A critical and comparative review of energy management strategies for microgrids. Elsevier Ltd Dec. 01, 2022. https://doi.org/10.1016/j.apenergy.2022.120028.

[27] Rathor SK, Saxena D. Decentralized energy management system for LV microgrid using stochastic dynamic programming with game theory approach under stochastic environment. IEEE Trans Ind Appl 2021;57(4):3990–4000. https://doi.org/10.1109/TIA.2021.3069840.
[28] Khan MW, Wang J, Ma M, Xiong L, Li P, Wu F. Optimal energy management and control aspects of distributed microgrid using multi-agent systems. Sustain Cities Soc 2019;44:855–70. https://doi.org/10.1016/j.scs.2018.11.009.
[29] Thirunavukkarasu GS, Seyedmahmoudian M, Jamei E, Horan B, Mekhilef S, Stojcevski A. Role of optimization techniques in microgrid energy management systems—a review. Energ Strat Rev Sep. 2022;43:100899. https://doi.org/10.1016/J.ESR.2022.100899.
[30] DCCEEW. *Australia's emissions projections 2022*. Canberra, 2022. Accessed: May 07, 2024. [Online]. Available: https://www.dcceew.gov.au/sites/default/files/documents/australias-emissions-projections-2022.pdf; 2022.
[31] ACIL ALLEN CONSULTING, "Emission Factors: Review of Emission Factors for Use in the CDEII," Apr. 2014. Accessed: May 07, 2024. [Online]. Available, https://aemo.com.au/-/media/files/electricity/nem/planning_and_forecasting/ntndp/2014/data-sources/20140411_emissions_report_v2.pdf.
[32] Independent Statistics and Analysis U.S. Energy Information Administration, "How much carbon dioxide is produced per kilowatthour of U.S. electricity generation?" Accessed: May 07, 2024. [Online]. Available, https://www.eia.gov/tools/faqs/faq.php?id=74&t=11.